UNIVERSITY OF OKLAHOMA

GRADUATE COLLEGE

SELECTION AND VALIDATION OF BIOSENSORS FOR A NOVEL HEALTHCARE ENVIRONMENT

A THESIS

SUBMITTED TO THE GRADUATE FACULTY

in partial fulfillment of the requirements for the

Degree of

MASTER OF SCIENCE

By

JESSE SCHETTLER
Norman, Oklahoma
2016

Downloaded from SHAREOK. Persistent Handle URL: https://hdl.handle.net/11244/34635

SELECTION AND VALIDATION OF BIOSENSORS FOR A NOVEL HEALTHCARE ENVIRONMENT

A THESIS APPROVED FOR THE
SCHOOL OF ELECTRICAL AND COMPUTER ENGINEERING

BY

_____
Dr. Hazem Refai, Chair

_____
Dr. Justin Feinstein

_____
Dr. Ali Imran

© Copyright by JESSE SCHETTLER 2016
All Rights Reserved.

Acknowledgements

Foremost, I would like to express my gratitude to my advisor, Dr. Hazem Refai. Thank you for your constant guidance, support, and encouragement throughout the research and writing of this thesis.

Great thanks go to my PI, Dr. Justin Feinstein, for making me a part of his lab and allowing me to embark on the unique journey that is float research.

I also greatly appreciate Dr. Ali Imran for serving on my committee and providing insightful comments and difficult questions.

Thank you Dad and Angela for giving me this opportunity and your continuous support, and thank you Mom for encouraging me to believe I can accomplish anything. A special thanks goes to my in-laws, Dick and Opal, for helping me pursue the will of God in every area of life. Thank you to my brothers, Dakota, Rylee, and Nathan, for always being such a great source of joy and excitement.

I am especially grateful towards my fellow students and labmates: Omar Al Kalaa, Naim Bitar, Ahmad Mayeli, Dr. Steve Green, Colleen Wohlrab, and Will Schoenhals.

Last but certainly not least, I would like to thank my wife Elizabeth for making this journey much more enjoyable and for ensuring that I never take myself too seriously. Also, thank you science. It has truly been a challenge to master you.

Table of Contents

Acknowledgements iv

List of Tables vii

List of Figures viii

Abstract x

Chapter 1: Introduction 1

Chapter 2: Related Work 7

Chapter 3: Selection and Modification of Devices 12

3.1 Selection Criteria 12

3.2 The Kinect 13

3.3 GENEActiv Original Accelerometers 16

3.4 The BioPatch 18

3.5 The QardioArm 21

3.6 The BrainStation 26

3.7 Rejected Devices 27

3.7.1 The EQ02 LifeMonitor 28

3.7.2 The iHealth and Withings Wireless Blood Pressure Monitors 31

3.7.3 The X4 Sleep Profiler 33

Chapter 4: Instrumentation Setup 35

4.1 Overall Setup 35

4.2 Time Sync Evaluation 41

4.2.1 Time Synchronization Protocol 41

4.2.2 RR-Interval-Based Synchronization of ECG Waveforms 45

4.2.3 Parallel-Port-Based Synchronization of ECG Waveforms 52
Chapter 5: Using a Neural Network to Calculate Cardiac Metrics 56
5.1 A Neural Network for Automatic Detection of R-peaks 56
5.1.1 Network Design 58
5.1.2 Training and Validation 60
5.1.3 Test Method and Results 63
5.2 Calculation of Cardiac Metrics 70
5.2.1 Heart Rate 70
5.2.2 Heart Rate Variability 72
Chapter 6: Measures of Movement – Stillness and Avoidance 76
6.1 Stillness 76
6.2 Avoidance 82
Chapter 7: Conclusion 84
References 86

List of Tables

Table 1. BioPatch Breathing Rates while Floating 21

Table 2. LifeMonitor Breathing Rates while Floating 30

Table 3. Biosensor Variables and their Frequencies 42

Table 4. Delay Stats for Matched Waveforms 52

Table 5. Accuracy of Neural Network 66

Table 6. Results of Testing 40-minute Signals 69

Table 7. Neural Network's SDNN and RMSSD Values 74

Table 8. Description of Movement Numbers 81

List of Figures

Figure 1. Open Float Tank 3

Figure 2. Enclosed Float Tank 3

Figure 3. Kinect App to Monitor Movement 14

Figure 4. Dome and Magnet System Used to Block IR Light 15

Figure 5. One Subject's Acceleration During a 90-minute Float Session 17

Figure 6. BioPatch ECG Signal at End of 90-minute Float Session 19

Figure 7. LimbO Cast Protector 22

Figure 8. Average Systolic Blood Pressure for 12 Subjects 25

Figure 9. Average Diastolic Blood Pressure for 12 Subjects 25

Figure 10. Comparison of One Subject's Heart Rate Values 26

Figure 11. BrainStation EEG Data 27

Figure 12. Silicone Putty Gaskets to Protect Electrodes 28

Figure 13. Heart Rate Comparison for One Subject 31

Figure 14. Noisy EEG Data from the X4 Sleep Profiler 34

Figure 15. GENEActiv Accelerometer Placement 37

Figure 16. Average Heart Rate Confidence for 42 Float Sessions 38

Figure 17. Average Breathing Rate Confidence for 42 Float Sessions 39

Figure 18. Overall Setup of Biosensors 40

Figure 19. Comparing Average Heart Rate with One Subject's Accelerometer Data 44

Figure 20. One Subject's Posture Changes during Two Float Sessions 45

Figure 21. Simultaneously Recorded ECG Waveforms 47

Figure 22. ECG Waveforms Shifted to Align R-peaks 49

Figure 23. RR-interval Plots 50
Figure 24. Synchronized Waveforms Using RR-Interval-Based Method 51
Figure 25. Parallel Port Prototype for Synchronization 53
Figure 26. ECG Waveform with Digital Signal 54
Figure 27. Synchronized Waveforms Using Parallel-Port-Based Method 55
Figure 28. Components of an ECG Signal 57
Figure 29. Neural Network Structure 59
Figure 30. Validation Results of Neural Network 63
Figure 31. Neural Network Flowchart 65
Figure 32. Clean ECG in Experiment 8 67
Figure 33. Baseline Drift in Experiment 7 67
Figure 34. T-wave Confusion in Experiment 5 68
Figure 35. No Detections in Experiment 10 68
Figure 36. Neural Network Heart Rate for One Float Session 71
Figure 37. BioPatch Heart Rate for One Float Session 71
Figure 38. BioPatch SDNN Values for One Float Session 73
Figure 39. Neural Network SDNN Values for One Float Session 73
Figure 40. Neural Network RMSSD Values for One Float Session 74
Figure 41. ROC Curves 79
Figure 42. Relative Activity Levels of Accelerometers 81

Abstract

Flotation tanks provide a unique environment for reducing the deleterious effects of stress on the human mind and body. As a result, biosensors capable of collecting objective physiological data during float sessions are needed to identify and quantify the resulting health effects. This thesis presents the selection and validation of off-the-shelf biosensors to investigate the physiological stress-reducing effects induced by this novel healthcare environment. The demands of the float environment required the biosensors to be wireless, waterproof, salt-proof, and minimally invasive. Interface and design modifications were made to the selected devices to ensure reliable operation in the unique conditions created by float tanks, and these modifications were tested for effectiveness in protecting the sensors, maintaining signal integrity, and reducing all forms of external sensory input that may detract from the float experience. As a result of the validation process, it was determined that the modified biosensors were capable of successfully recording movement, electrocardiograph (ECG), respiration, electroencephalograph (EEG), and blood pressure during float sessions.

This thesis also investigated time synchronization and the analyses of biosensor outputs as they pertain to float research. A method to ensure time synchronization among sensors was developed and tested against an industry-leading physiological recording device to verify the accuracy of the biosensors' timestamps. Additional experiments among sensors were conducted to further validate the technique and illustrate that a transient event can be identified across multiple data streams. A neural network was

designed to facilitate the calculation of cardiac metrics such as heart rate and heart rate variability, and the results were analyzed to determine which methods provide the most useful information for float research. Data obtained from two accelerometer devices was also examined to determine optimal cut-points for classifying movement within the float tank, and measures of stillness and avoidance behavior were characterized. The proposed biosensors and methods were found to reliably and accurately measure changes in physiological variables during float sessions. This thesis documents the first successful implementation of collecting continuous physiological data during the float experience.

Chapter 1: Introduction

Float tanks, also referred to as isolation tanks, are lightless, soundproof tanks in which people float effortlessly in a dense salt water solution warmed to skin temperature. This unique environment reduces external sensory input (including visual, auditory, tactile, proprioceptive, and thermal sensory input) and is often described as sensory deprivation; however, this term can be misleading. Although float tanks reduce external sensory input, they often enhance internal sensory input, especially signals arising from the heart and respiration. This creates a peaceful meditative environment that naturally induces a state of relaxation. Objectively measuring this relaxation response has remained elusive, and past flotation research has failed to identify biosensors capable of recording signals in this unique environment.

Float tanks come in various sizes and designs, but the basic components are the same. The two tanks used in this study are depicted in Figures 1 and 2 (Floataway, Norfolk, UK). Each circular pool is 2.5 m in diameter and contains roughly 1.25 kL of water mixed with 900 kg of Epsom salt (magnesium sulfate). This dense solution allows a person to float near the surface when in a supine position. The air in the rooms and water in the tanks are heated to skin temperature (34.5 ^{o}C), and the rooms in which the tanks are built are soundproof and devoid of light. These aspects of floating are responsible for the aforementioned reduction of external sensory input.

Research involving float tanks and sensory deprivation began in the 1950s but lacked technology capable of thoroughly investigating the resulting health effects [1], [2]. As a result, the field has remained relatively stagnant for the past half-century. The recent development of easy-to-use biosensors and the increased popularity of recreational floating have driven researchers and float tank entrepreneurs desiring to promote their businesses to revisit this topic of study. Early float research revealed that this therapeutic experience lowers levels of stress [3], [4], anxiety [5]–[7], and blood pressure [8], [9]. Today, people anecdotally report that floating alleviates chronic pain, depression, and eating disorders. Such reports have prompted business owners to add float tanks to their existing spa facilities, and clinical neuropsychologists are experimenting with float tanks as a type of therapy for reducing the negative effects of stress and anxiety.

Since floating is returning as a form of treatment in a number of recreational and healthcare settings, biosensors that collect empirical data and examine float therapeutics are essential for accurately quantifying the resulting effects. Given the float tank's unusual conditions, such devices must be waterproof and noncorrosive in the presence of salt. Furthermore, since floating is intended to minimize external sensations, devices must be minimally invasive and free of wires and attachments when possible. A form of wireless, real-time data transmission and viewing is also often desired to monitor participants during a float session.



Figure 1. Open Float Tank



Figure 2. Enclosed Float Tank

The objective of this thesis was to select and validate biosensors and their outputs for the study of float research. This involved:

- Using selection criteria to select and modify devices.
- Validating the general usability of devices in the float environment.
- Analyzing device outputs to develop optimal metrics for float research.

For the selection of devices, off-the-shelf biosensors were chosen opposed to custom-made devices available only to research institutes. Using readily available devices facilitates collaboration between researchers and float businesses where the increased resources of the businesses can be utilized to conduct studies on a larger scale. The selected devices in this study collect movement, electrocardiogram (ECG), respiration, electroencephalogram (EEG), and blood pressure data. Many of the wearable biosensors available to the public do not meet requirements necessitated by the float tank environment, so this thesis developed simple design modifications that can be easily implemented by other researchers and entrepreneurs alike.

Following the modification process, initial testing was performed to determine the devices' suitability and usefulness in float research. Various experiments were conducted to ensure that the biosensors operate in the float environment without experiencing physical damage or loss of data. Other tests investigated whether or not the proposed modifications altered the output of a device. The biosensors were also validated as a system. Protocols and tools for synchronizing devices were developed and analyzed to determine how data from separate devices can be compared.

A comprehensive study of the devices' outputs was then performed once the biosensors had been validated. Various cardiac metric algorithms and methods were analyzed to determine how to provide full access to the most useful information for float research. Devices that record movement data were compared to identify redundant information, and cut-points were optimized to classify movement.

The following list summarizes the contributions of this thesis:

- Identified selection criteria and utilized it to select off-the-shelf biosensors for float research.
- Developed easily reproducible modifications to devices to prevent physical damage, data loss, and excessive sensory input.
- Validated the ability of each device to collect usable data during float sessions and characterized the effects that modifications have on the data.
- Constructed a method of time synchronizing biosensors to enable the comparison of data from separate devices.
- Designed a neural network to automatically detect R-peaks in ECG data.
- Compared various cardiac metrics to determine which algorithms provide the most useful information for float research.
- Analyzed data from multiple movement-tracking devices to identify redundancies and create cut-points for classification of movement.
- Defined stillness and avoidance behavior to facilitate the study of movement.

The remainder of this thesis is organized as follows. Chapter 2 presents an overview of related work. Chapter 3 details the biosensor selection and modification processes, along with validation of the usability of devices in the float environment. The instrumentation setup and time synchronization procedures are described in Chapter 4. Chapter 5 describes the neural network and provides an analysis of cardiac metrics and algorithms, identifying which are most useful for float research. Movement-tracking devices are compared in Chapter 6 to determine redundant devices and develop cut-

points for accurate classification of movement. Chapter 7 offers a conclusion of the thesis and provides directions for future research.

Chapter 2: Related Work

The work presented in this thesis built upon existing float studies and research involving the testing of devices and their outputs. This chapter presents an overview of related work and discusses physiological monitoring, various validation methods, and time synchronization.

Previous float studies implemented measurement devices to examine the physiological effects of floating. The most common variable recorded was blood pressure. In an attempt to capture long-term effects, Fine et al. measured blood pressure prior to float sessions and in follow-up appointments [8]. Others [9]–[14] recorded blood pressure before and after each float to capture immediate results. In [15], [16], the authors collected blood pressure data only on non-float days, and another study measured blood pressure three times a day during the entire course of the experiment [17]. The literature certainly reveals that floating can decrease blood pressure, but no studies have attempted to monitor blood pressure continuously throughout the duration of float sessions. Thus, the changes that occur to blood pressure during the course of a float session are still largely unknown.

Another common physiological variable studied in early float research is ECG. In [5], Forgays et al. used electrodes wired to a Narco Bio-Systems FM-1100 E2 transmitter and a matching biotelemetry FM-1100-7 receiver to record ECG before, after, and during float sessions; however, the authors discarded 30% of the data due to signal loss.

In a later study, they recorded ECG only before and after the float sessions [18]. In his master's thesis, Steel successfully recorded ECG during floats to examine changes in T-wave amplitude and heart rate [19]. He also tried to measure EMG but lost the data due to low signal-to-noise ratio. The authors of [20] measured heart rate before and after knee exercises and float sessions but not during the float sessions themselves.

A few researchers recorded EEG during float sessions. One study used electrodes covered with a "mighty dry" diaper and surgical cap to continuously measure EEG without signal loss [21]. Fine et al. employed an Autogen 120 EEG device with wired electrodes to record average frequency, average amplitude, and percent time in filter range [22]. One electrode was placed on the forehead, while the other two were attached to nasal cartilage.

Forgays et al. also measured breathing rate and frontalis muscle movement, but no analysis was presented [5]. No studies have thoroughly investigated the effects of floating in regards to breathing rates and body movement.

Most wireless and mobile health sensors have gone through clinical testing to receive certification and FDA approval. When modifications are made to these devices to ensure compatibility with the float environment, additional validation is necessary. The Association for the Advancement of Medical Instrumentation (AAMI) often develops standards used in clinical validation. The standards stipulate test conditions, number of

subjects, and pass-fail criteria [23]–[25]. Such protocols can be adapted to validate modified devices.

Other health devices, such as accelerometers that measure movement, do not require clinical validation. Instead, researchers often compare them to other devices or reference measures to determine accuracy. In [26], Esliger et al. used a mechanical shaker, a metabolic gas analyzer, and two additional accelerometers to validate the device under study. Using the shaker, they oscillated the accelerometers at specific frequencies and amplitudes and calculated standard deviation, coefficient of variation, and the Pearson product-moment correlation to determine the validity and reliability of the raw acceleration values. They then employed the gas analyzer to measure VO_2 during graded exercise, which was used to compute Pearson product-moment correlations for each accelerometer. Receiver-operator curves (ROC) were then analyzed to determine optimal cut-points to accurately classify activity levels using the accelerometers. The authors of [27] later tested these cut-points, again making use of oxygen uptake measurements for the analysis.

Another study similarly compared two accelerometers by oscillating them with an orbital shaker [28]. The authors took this work a step further by developing models to classify activity levels from acceleration values. They attempted to train the models using data from one accelerometer and then apply them to data from the other. Classification accuracy decreased significantly when models were applied to data from a different device.

In the same way that movement-based metrics are often studied instead of raw acceleration values, cardiac metrics are analyzed to ensure accuracy and determine their meanings. In [29], heart rate variability (HRV) is defined along with various methods used to calculate it. The authors explain the aspects of HRV that each method emphasizes and propose guidelines for ensuring accurate HRV determinations. Such an analysis is necessary in float research to ensure the acquisition of metrics that yield the most useful information.

Validating devices and their operation as a system greatly depends on time synchronization. For slow-changing physiological variables, it may be sufficient to use local timestamps to compare data between devices. For other variables, a more precise method is required. When the device being used is connected to the Internet, the Network Time Protocol (NTP) described in [30] ensures the precise time synchronization necessary when dealing with fast-changing variables. An NTP server regularly synchronizes clocks in its network to within a few milliseconds of Coordinated Universal Time (UTC).

Unfortunately, many mobile health devices are not connected to an NTP server. These devices synchronize their real-time clocks (RTCs) to a computer when connected, but the RTCs have only one-second precision. Synchronizing these clocks with greater precision usually requires injecting a common signal into each data stream. Such a process is described in [31] by BIOPAC, a leader in the physiological data acquisition industry. BIOPAC injects a digital signal into its data streams in order to synchronize

stimulus presentations with multiple response recordings. Float research requires a similar method for experiments that measure fast-changing variables and response times.

Chapter 3: Selection and Modification of Devices

The process of choosing biosensors for use in float research began with defining selection criteria. This chapter details these criteria and the resulting procedures used for selecting and modifying devices. This work focused on biosensors that monitor movement, ECG, respiration, EEG, and blood pressure since these measures are strong indicators of relaxation and are commonly studied in the literature. Each selected device was tested to determine its usability in the float environment.

3.1 Selection Criteria

The conditions of the float experience impose unique requirements on physiological devices used in float research. Float tanks contain an extremely dense salt-water solution and allow participants to float around unrestrained. The purpose of the environment is to reduce external sensory input. Based upon these characteristics, biosensors utilized in float research must be:

- Waterproof
- Non-corrosive in the presence of salt
- Free of wires and attachments
- Minimally invasive in terms of auditory, visual, and tactile stimulation

In addition to these requirements, it is desirable for the devices to provide real-time data streaming to enable participant monitoring and provide biofeedback during float experiments. Unfortunately, few off-the-shelf devices meet these criteria. Devices that

meet these standards the closest must be identified and then modified to overcome their limitations. After reviewing various biosensors on the market, devices were selected for validation according to the selection criteria.

3.2 The Kinect

The Kinect (Microsoft, Redmond, WA) was initially chosen as the primary method of monitoring movement. The Kinect uses an infrared (IR) camera to noninvasively obtain depth images even in the absence of light, and the images are decomposed to provide skeleton joint points as xyz-coordinates [32]. The Kinect has been successfully used to analyze gait biometrics [33] and to track head motion [34]. It can be mounted above the float tank to avoid water damage, and it does not introduce any auditory or tactile stimuli into the float environment. The Kinect comes with many sample apps that allow users to display incoming RGB, depth, and skeletal data in real-time. Microsoft also provides a free software development kit (SDK) to create custom apps. For this work, the SDK was used to develop a Windows Forms application that displays joint points as a connected skeleton. The app also calculates the number of limb movements and the amount of time spent moving as illustrated in Figure 3. Since subjects usually float without clothing, the Kinect's RGB data stream is disabled to protect participant privacy. Only skeletal data is collected and viewed.

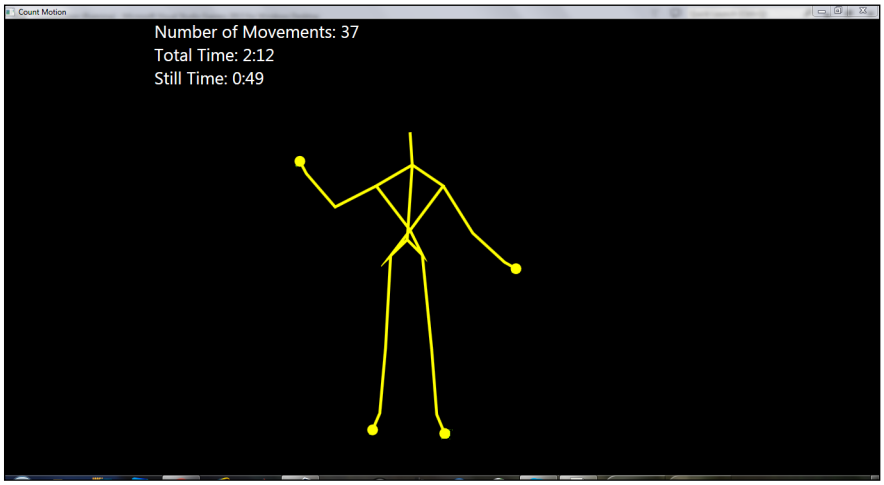

Figure 3. Kinect App to Monitor Movement

The Kinect's limitations are that the IR light is visible to the human eye and skeleton tracking does not work when a participant is upside down. A spectrum analyzer revealed that the IR light has a single wavelength of 830 nm, meaning that filters would completely block the light and prevent motion detection. As an alternative solution, the Kinect was covered with a clear dome, and pairs of magnets were placed on each side of the dome as illustrated in Figure 4. Magnets on the outside of the dome are held in place by magnets on the inside of the dome, and they can slide to any position to block the IR light from a participant's view without negatively affecting movement tracking. In order for this method to work, a foothold system must be used to keep participants in a constant position. This is physically invasive but ultimately prevents participants from rotating in the tank and ensures that skeletal data can be collected. Certain float experiments require a constant head position anyway, so the Kinect can be employed in those studies without increasing the overall level of invasiveness.

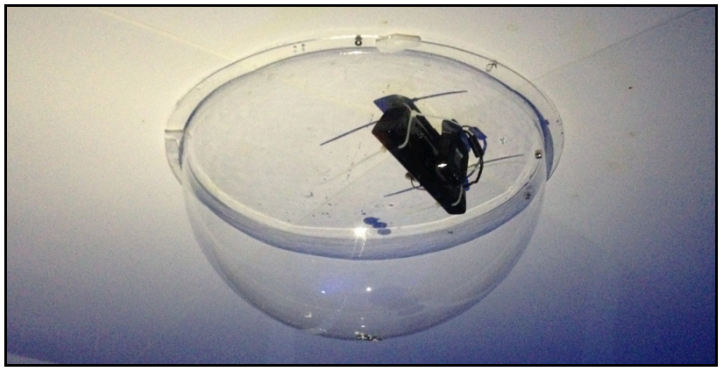

Figure 4. Dome and Magnet System Used to Block IR Light

The Kinect was tested with three subjects to validate its usability in the float environment. It was mounted above the closed float tank and covered with the dome system previously described, and the devised foothold system was employed to place the participant's head in a specific location to block the IR light from view. Notably, the foothold system can be adjusted in one inch increments, and the magnets can slide anywhere on the dome to ensure the IR light is blocked from view for participants of various heights.

After positioning a participant, the skeleton tracking application was initialized, and data collection commenced. The Kinect locates an individual based on his or her distance from the background, so it had difficulty distinguishing an individual's body from the water in the tank. To remedy this, participants were instructed to lift their arms out of the water towards the camera while at the same time moving their legs back and forth. These movements created distance between the subject and the water and aided the Kinect in locating the participant, and the app successfully displayed the resulting skeleton. Alternatively, the Kinect can be switched from default mode to seated mode.

This causes the Kinect to track only the upper body and uses movement to initially locate the participant instead of distance. Experimental results revealed that tracking in seated mode results in quicker detection. After being located, the participants were asked to move their limbs to specific positions to test whether or not the skeleton accurately reflected those positions. The skeleton mirrored all three participants' movements without ever losing their locations.

The Kinect was also tested without using the foothold, dome, and magnets. As mentioned previously, the Kinect was unable to accurately track someone upside down. If a participant floats into this position, the displayed skeleton becomes severely disfigured until the participant returns to the upright position. When floating without the dome and magnets, the three participants stated that the IR light was not noticeable as long as their eyes were closed. The proposed modifications can be implemented flexibly to align with various experimental designs.

3.3 GENEActiv Original Accelerometers

As a second tool for tracking limb movements, the GENEActiv Original accelerometer (GENEActiv, Cambridgeshire, UK) was selected. This device records raw acceleration in the xyz-directions and is waterproof. It can be somewhat invasive, especially to participants not accustomed to wearing wristwatches, but is a good alternative to the Kinect when movement data is needed for an entire float session that does not use the

foothold system. The device stores data locally and cannot transmit wirelessly. No modifications were made to this device.

GENEActiv accelerometers were shown to be both reliable and valid in [26], [28]. To begin validating the devices in float tanks, 11 participants wore a GENEActiv accelerometer on each wrist during 2 90-minute floats. These experiments confirmed that the watches are not damaged by the salt solution and are waterproof. The collected data reflected movement occurring within the float sessions as depicted in Figure 5, and Chapter 4 presents some of this data as it pertains to time synchronization. Also, Chapter 5 uses this data as a reference to develop cut-points for another device. Initial testing verified that GENEActiv Original accelerometers are viable for use in the float tank environment.

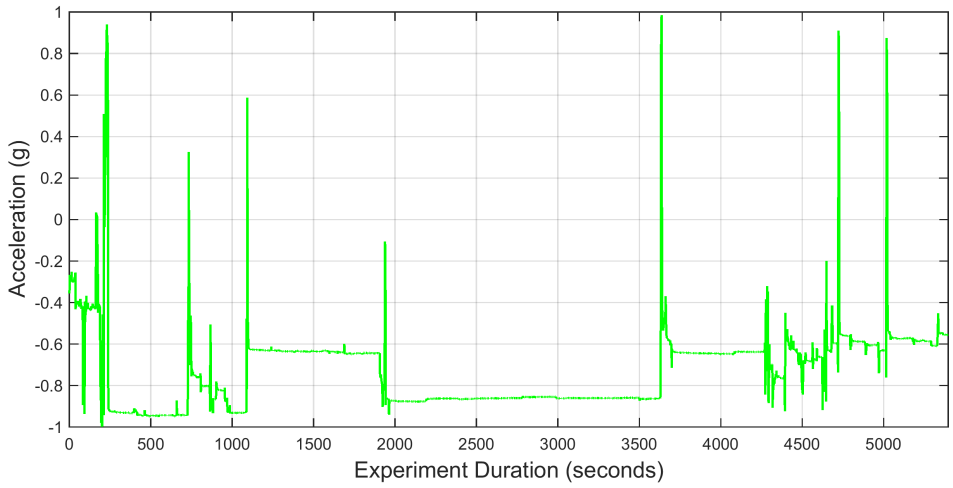

Figure 5. One Subject's Acceleration During a 90-minute Float Session

3.4 The BioPatch

The BioPatch (Medtronic, Fridley, MN) consists of a small physiological monitoring module that attaches to the chest using standard ECG electrodes. It records ECG and breathing waveforms without the use of a chest strap by implementing a novel and proprietary measure of impedance, making it much less invasive than similar devices on the market. It also measures acceleration, posture, and skin temperature. The BioPatch stores data locally and can transmit one-second vitals via Bluetooth for real-time monitoring. The BioHarness, a similar device produced by the same company, uses a chest strap with embedded electrodes to measure the same variables. The validity and reliability of the BioHarness were proven in [35]–[37], and the results are applicable to the BioPatch since it uses the same algorithms.

Although a participant's chest usually remains above the water in a float tank, certain movements can cause the salt solution to reach the BioPatch electrodes and ruin the signal. The recent development of hydrophobic carbon electrodes that provide clean ECG signals in water-immersed conditions could easily solve this problem [38], but the BioPatch itself is not waterproof. Thus, Tegaderm (3M Healthcare Ltd., Loughborough, UK) is used to cover the BioPatch and prevent signal loss and physical damage in worst-case scenarios. The BioPatch also has flashing lights that must be covered with tape to ensure the device does not provide unwanted visual stimulation to participants.

To determine whether or not the BioPatch can record a usable ECG signal in the float environment, it was tested with 21 subjects during 90-minute float sessions. In all 21 tests, the BioPatch successfully recorded ECG without signal loss or physical damage. A valuable characteristic of the BioPatch software is that it displays a heart rate confidence value between 0 and 100 in real time to signify whether or not the ECG signal is corrupted. As part of this study's protocol, it is required that the heart rate confidence value reaches 100 before a participant can begin the float session, and the value is monitored as the participant enters the tank. When necessary, a participant can be asked to exit the tank and readjust the BioPatch and Tegaderm if the confidence value drops. In this way, it is ensured that the BioPatch successfully records ECG. An example signal taken from the end of a 90-minute float is depicted in Figure 6.

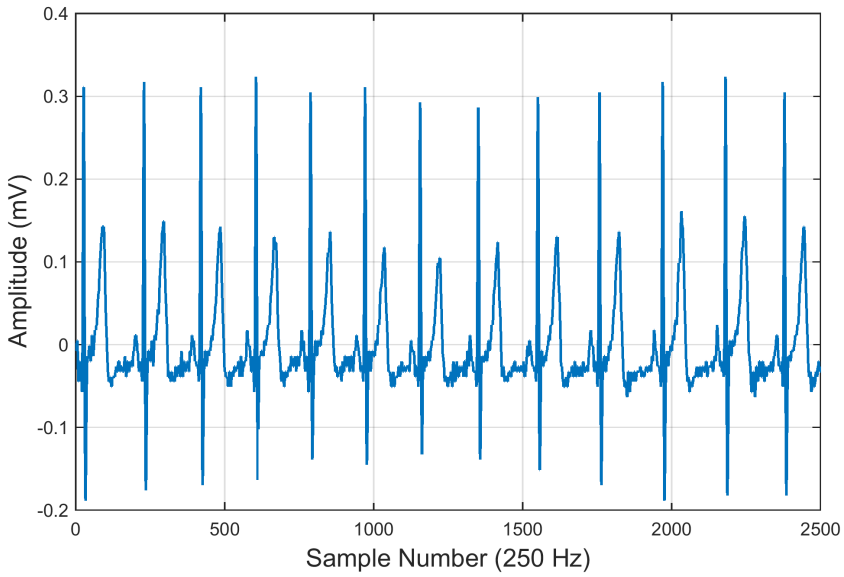

Figure 6. BioPatch ECG Signal at End of 90-minute Float Session

Along with ECG, the BioPatch successfully recorded posture, acceleration, skin temperature, and breathing rates during the 21 float sessions. The posture data is presented in Chapter 4 to illustrate time synchronization and event identification. Chapter 5 analyzes the acceleration data to determine optimal cut-points for movement classification.

The accuracy of the BioPatch's breathing rate values was evaluated in an additional experiment. A metronome was set to rates between 3 and 30 beats per minute, and participants were instructed to match their breathing to the rhythm while floating. When participants were able to sustain a breathing rate of 4 breaths per minute, the BioPatch accurately detected it as revealed in Table 1. Some participants were not able to maintain the lower breathing rates for the entire test duration. For those who did, the BioPatch was able to distinguish between most breathing rates between 4 and 30 breaths per minute. Since this covers the typical breathing values expected in float research, it was determine that the BioPatch is a valid biosensor to monitor breathing during float sessions.

Table 1. BioPatch Breathing Rates while Floating

Metronome Rate (Beats per Minute)	Average Breathing Rate (Breaths per Minute)
10	9.95
15	14.27
5	5.37
7	7.13
3	4.83
5	4.95
4	4.12
6	5.72
20	18.40
30	28.61

3.5 The QardioArm

After a testing a few different blood pressure devices, the QardioArm wireless blood pressure monitor (Qardio, Inc., San Francisco, CA) was selected to measure blood pressure and heart rate. This device uses Bluetooth Smart, which performs well when establishing and maintaining connections. The QardioArm pairs with and is controlled by a smart phone or tablet. After a measurement is taken, the controlling device stores the data locally and also uploads the information to a cloud server. Data can be downloaded as either a CSV or Excel file, and then loaded into an external application for further analysis. The QardioArm is smaller and quieter than other blood pressure monitors and stays powered on for 15 minutes before automatically shutting off. Other devices turn off within two to five minutes.

The QardioArm is not waterproof and thus cannot survive in the float environment. To solve this issue, LimbO cast protectors (Thesis Technology, Hampshire, UK) designed to keep arm and leg casts dry when an individual is taking a shower or swimming in a pool were purchased. The LimbO cast protector is placed over the blood pressure device and participant's arm to create a watertight seal as shown in Figure 7. The QardioArm's smaller size again offers a benefit in that it can more easily fit into the LimbO without applying additional pressure to a participant's arm.

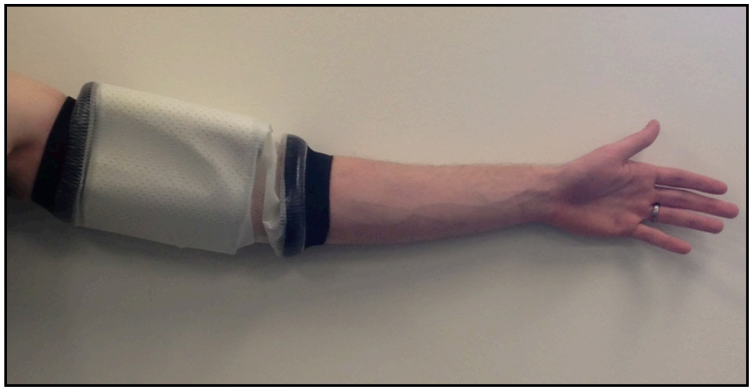

Figure 7. LimbO Cast Protector

The QardioArm was clinically validated according to [23], [24], so initial tests were aimed at determining whether or not the device could survive in the float environment and maintain its Bluetooth connection. For 3 subjects, the device was triggered at 10-minute intervals. The QardioArm successfully provided blood pressure and heart rate data at each interval during the float sessions, and the LimbO prevented water from damaging the device. Participants also reported that the Qardio Arm felt less invasive due to its smaller size.

A study in the literature compared the QardioArm to other smartphone compatible blood pressure monitors and found that the QardioArm's mean diastolic blood pressure was 3.955 mmHg higher than that of one of the other devices [39]. Other differences were not statistically significant, and no standard reference device was used. To further investigate these mean differences and determine whether the LimbO cast protector adds to them, the QardioArm was tested against a reference device with 12 subjects. For each subject, six measurements were taken with the QardioArm, the QardioArm covered with a LimbO, and the CASMED 740 Select (CAS Medical Systems, Inc., Branford, CT) for a total of 18 measurements per subject. Each participant was given a five-minute rest period before measurements began, and the order of devices was selected to produce two tests for each of the six possible orders. One minute of rest was given between each measurement, and six measurements were taken with one device before switching to the next device.

As Figure 8 reveals, the QardioArm's mean systolic blood pressure was 5.723 mmHg higher than the reference device, and this difference increased to 7.250 mmHg when using the LimbO cast protector. For mean diastolic blood pressure, the QardioArm measured 1.611 mmHg higher than the reference without the LimbO and 4.000 mmHg higher with the LimbO. The standard deviation of systolic blood pressure was 7.708, 9.979, and 7.345 mmHg for the QardioArm with LimbO, QardioArm without LimbO, and reference device, respectively. For diastolic blood pressure, the standard deviations were 8.179, 9.157, and 6.455 mmHg. This suggests that the QardioArm is best suited for measuring blood pressure differences instead of raw values. The differences in

average values mean that the QardioArm should not be used to group participants into hypertension categories, but the similar standard deviations mean that the QardioArm should measure changes in blood pressure values as effectively as the reference device. Thus, the QardioArm can be used to compare blood pressure differences throughout and between float sessions.

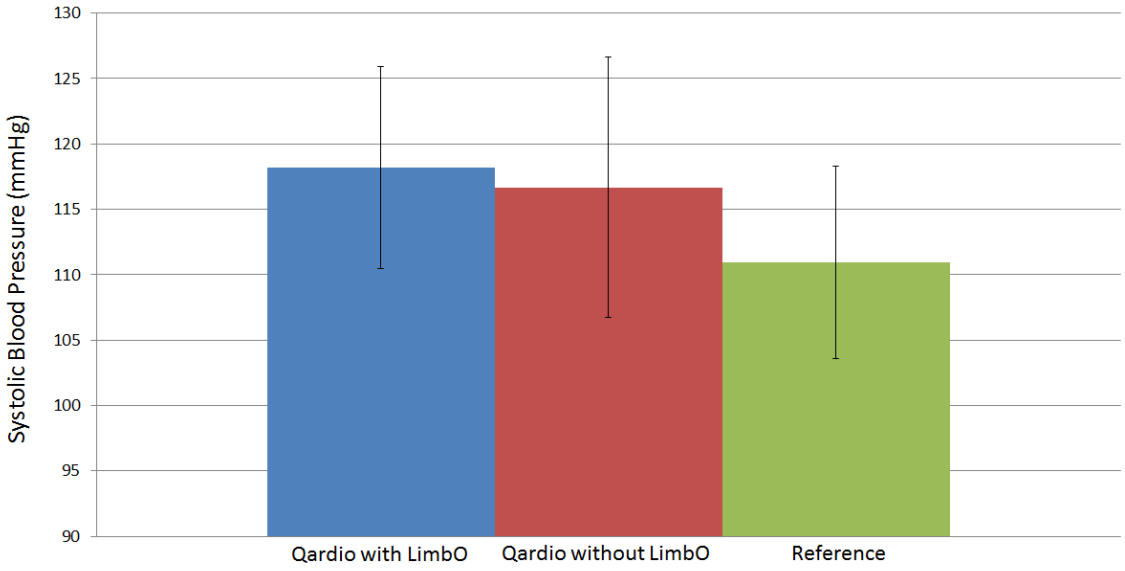

Figure 8. Average Systolic Blood Pressure for 12 Subjects

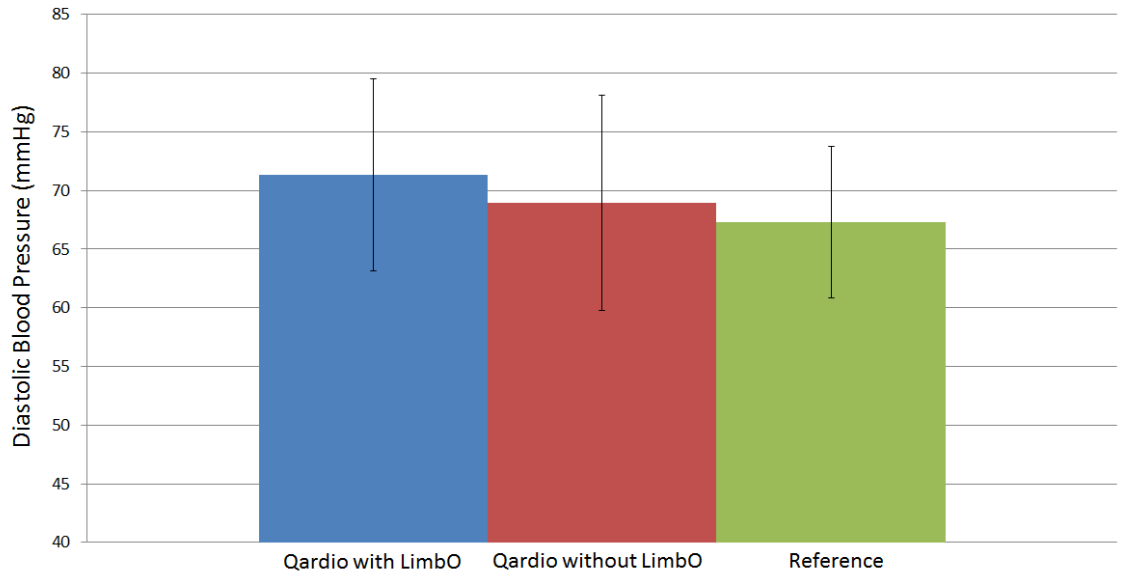

Figure 9. Average Diastolic Blood Pressure for 12 Subjects

The heart rate values of the QardioArm were compared to those of the BioPatch blood pressure device, and the results depicted in Figure 10 reveal that the two devices show

similar values and patterns. Differences are most likely due to the fact that the QardioArm takes a measurement at a single point in time, making it more susceptible to extreme changes and outliers. The QardioArm can be configured to take two or three measures and report the average to decrease this variability.

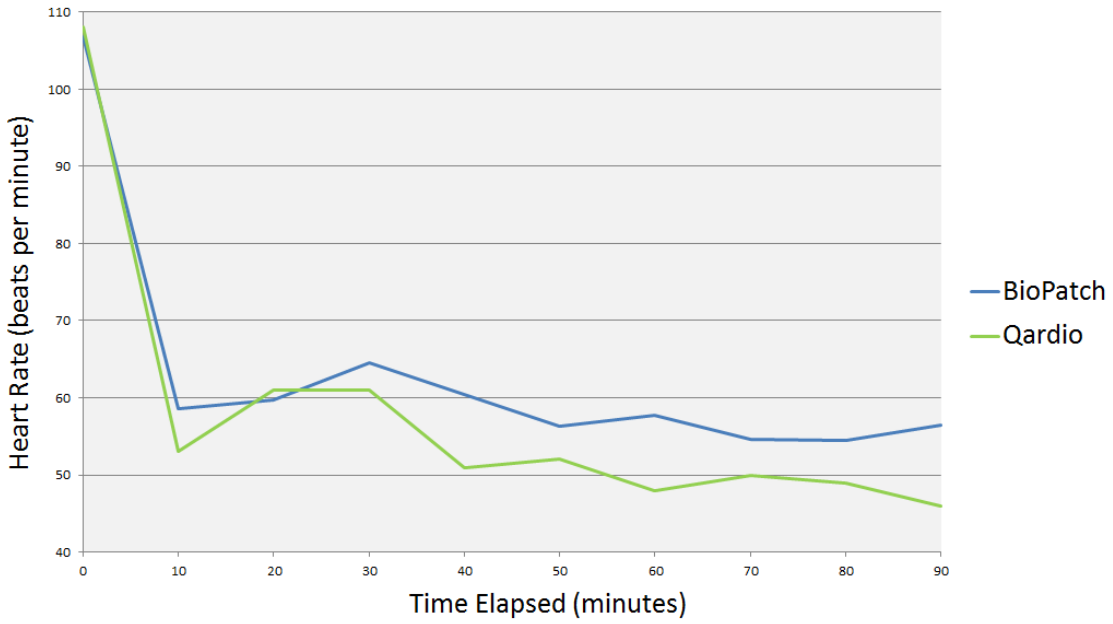

Figure 10. Comparison of One Subject's Heart Rate Values

3.6 The BrainStation

The BrainStation (Neuroverse, Inc., San Diego, CA) consists of a small electronics module and sticker electrodes that attach to the forehead to record a participant's EEG signal, which it transmits to a connected smartphone or tablet via Bluetooth. The data is then uploaded to a cloud server for further analysis. The BrainStation is not completely waterproof, but utilizes gold-plated electrodes embedded in a Tegaderm film to obtain

clean EEG data [40]. An additional Tegaderm patch is applied to the device to protect it from water during float sessions.

Since the BrainStation was discovered at the end of this research, only initial usability tests were conducted. The device was tested with 5 subjects while floating for 60 to 90 minutes. Initial testing verified that the Tegaderm protected the device and that EEG was recorded throughout the float sessions without signal loss while subjects were fully immersed in the float environment with ears under water. Figure 11 depicts an example of the EEG data collected during a 90-minute float.

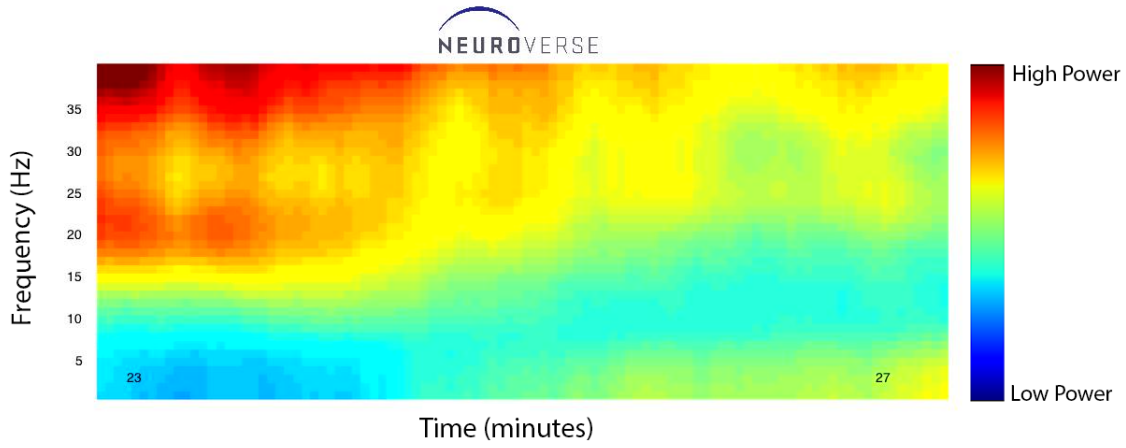

Figure 11. BrainStation EEG Data

3.7 Rejected Devices

Other biosensors initially selected for this research did not pass general usability tests. The following subsections describe these devices and the limitations that eliminated them from being used in float research.

3.7.1 The EQ02 LifeMonitor

The EQ02 LifeMonitor (Equivital, Inc., Cambridge, UK) was the original choice to obtain ECG and respiration data. This device also records body temperature, skin conductance, and acceleration. It has been used to monitor military performance [13], to acquire real-time data for preventive medicine [14], and to analyze physiological changes during high-altitude parachute jumps [15]. The LifeMonitor is composed of a belt containing embedded electrodes, a string gage, and sensors connected to a Sensor Electronics Module (SEM) for mobile monitoring. The system was advertised as waterproof and capable of transmitting data in real time.

To obtain clean ECG signals free of noise in the float environment, the LifeMonitor's electrodes must be isolated from the salt solution as much as possible. To this end, protective gaskets were fashioned out of silicone putty and placed around the electrodes as shown in Figure 12. The putty creates a watertight seal between the body and the electrodes, and electrode gel was applied to the electrodes to improve signal strength.

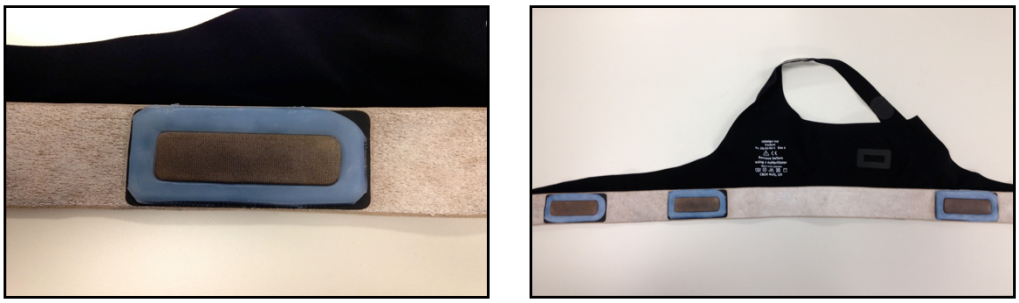

Figure 12. Silicone Putty Gaskets to Protect Electrodes

To test this solution, 5 participants floated for 60-minute sessions while wearing the LifeMonitor. Initially, two of the participants soaked the electrodes upon entering the tank, causing complete loss of the ECG signal. After training individuals to carefully enter the tank, three were able to keep chest electrodes relatively dry. Even in these situations, the signal became attenuated as more salt water saturated the fabric of the chest strap and eventually the electrodes. At the end of most sessions, the ECG signal was too weak to accurately calculate heart rates.

To determine breathing measurement accuracy, the Equivital LifeMonitor was tested in a reclined chair and in the float tank with three subjects. For each test, participants were asked to match their breathing to the rhythm of a metronome. On one tone the participant was instructed to inhale, and on the next he or she was instructed to exhale. The LifeMonitor breathing rate measurements were then compared to the expected breathing rates to determine the accuracy. Results showed that Equivital calculations are accurate when participants breath between 6 and 25 breaths per minute. Outside this range, participants have difficulty maintaining the prescribed rate, making it difficult to determine whether the LifeMonitor is reporting incorrect values or the participants are breathing at the wrong rates. Table 2 displays the results of a participant breathing to the beat of a metronome at different rates for three-minute periods during a float session. As can be seen, breathing rates below six breaths per minute do not match the metronome rates. Since normal resting rates vary from 12 to 25 breaths per minute, this limitation should not be a problem in most experiments.

Table 2. LifeMonitor Breathing Rates while Floating

Time Elapsed (Seconds)	**Average Breathing Rate (Breaths per Minute)**				
30	9.95	7.45	7.30	5.15	3.00
60	10.15	8.45	7.50	4.00	5.00
90	9.90	8.45	5.95	4.50	4.50
120	10.00	7.25	5.50	7.30	2.75
150	9.90	8.15	5.65	8.70	3.65
180	9.86	8.00	5.96	6.26	3.46
Metronome Rate (Beats per Minute)	10	8	6	4	2

Heart rates calculated by the LifeMonitor were also compared to those measured by two wireless blood pressure monitors described later. Figure 13 shows that the LifeMonitor and Withings device yield similar results, with the exception of three outliers recorded by the LifeMonitor. These three extreme measurements reinforce the fact that the salt water more negatively affects the LifeMonitor than other devices.

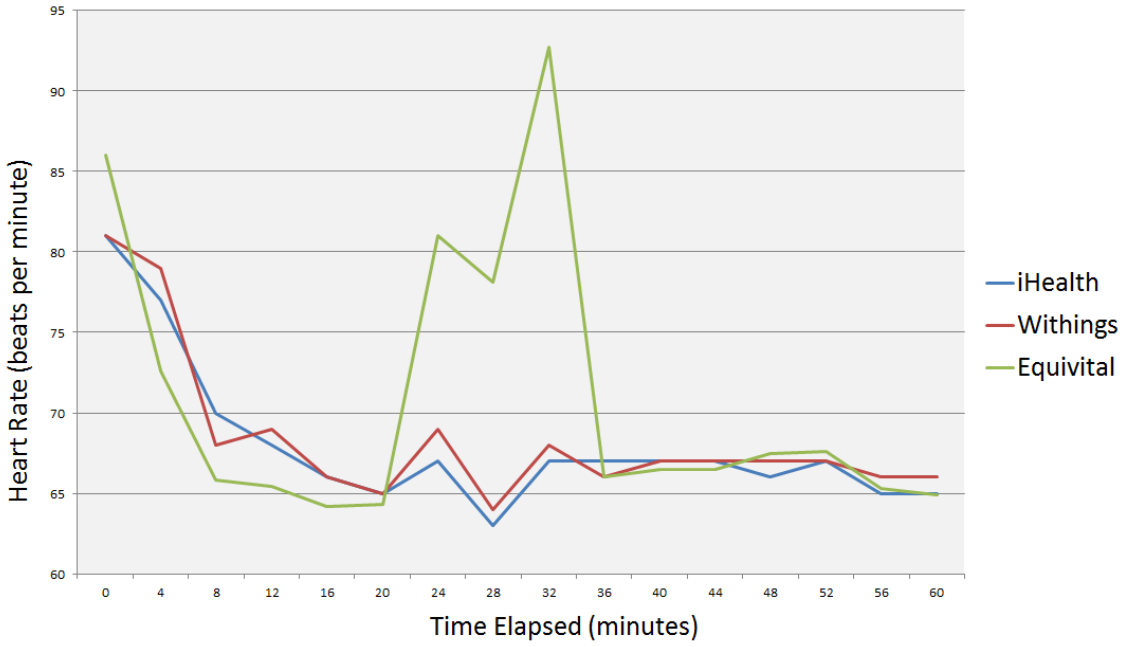

Figure 13. Heart Rate Comparison for One Subject

Although the LifeMonitor is wireless and accurately measures breathing rates, its inability to measure ECG during float sessions makes it unusable for this research. This device is better suited for studies examining breathing rates and the associated waveforms.

3.7.2 The iHealth and Withings Wireless Blood Pressure Monitors

The iHealth (iHealth Labs, Inc., Mountain View, CA) and Withings (Withings, Issy-les-Moulineaux, FR) wireless blood pressure monitors operate similarly to the QardioArm but automatically turn off after two to five minutes of not being used. This requires measurements to be taken much more frequently during float experiments, which is more invasive and disruptive to subjects. In contrast to the QardioArm and Withings

devices, the iHealth blood pressure monitor does not use Bluetooth Smart. The older version of Bluetooth prevents it from maintaining a connection during the float sessions, so it was quickly discarded in this work.

The accuracy of the Withings wireless blood pressure monitor was previously validated in [18], so this study tested the device to evaluate whether or not it could collect data during 60-minute float sessions without loss of connection or automatically turning off. During these tests, participants were asked to float with the blood pressure device and LimbO cast protector while blood pressure and heart rate were measured at four-minute intervals. Since the Withings device turns off after 2 minutes of non-use, the device was triggered from a tablet in 2-minute intervals. For every other trigger, the test was manually canceled from the tablet before the blood pressure cuff began inflating and interrupting the participant. Using this method, data was collected for the full duration of the float sessions, but the repeated triggering of the device was tedious and cumbersome to the experimenter.

Another drawback of the Withings device is its size. Compared to the QardioArm, it is much larger and more difficult to fit inside the LimbO without it applying additional pressure to a subject's arm. Due to this and the quick shutoff timer, the Withings device was rejected in favor of the QardioArm.

3.7.3 The X4 Sleep Profiler

For collecting EEG data, the X4 Sleep Profiler (Advanced Brain Monitoring, Inc., Carlsbad, CA) was initially chosen. Because Advanced Brain Monitoring specifically modified this device for float environments, initial alterations were not necessary. The X4 has an electronics module for data storage and transmission. The module is attached to a band with three electrodes, and the electrodes are placed on a participant's forehead during a float session. Although other EEG devices on the market include an additional number of electrodes, the technology fails to maintain a watertight seal and prevent signal loss. The X4 is water-resistant and can be configured to transmit data wirelessly in real-time.

The accuracy of the X4 in dry environments was validated in [16] and [17]; therefore, only the device's ability to operate in the float environment and avoid signal loss was evaluated. The device was tested with and without a head pillow. The head pillow kept the participant's head and the X4 out of the water, resulting in a protected device. Without the use of a head pillow, water damaged the device on two occasions and significant signal loss occurred. Few tests provided usable data without the use of a head pillow. Unfortunately, even with the head pillow most participants could not keep salt water from reaching the electrodes on their foreheads. This resulted in noisy EEG signals as illustrated in Figure 14. Since more than 50% of experiments failed to yield usable data, the X4 was abandoned in search of a new device.

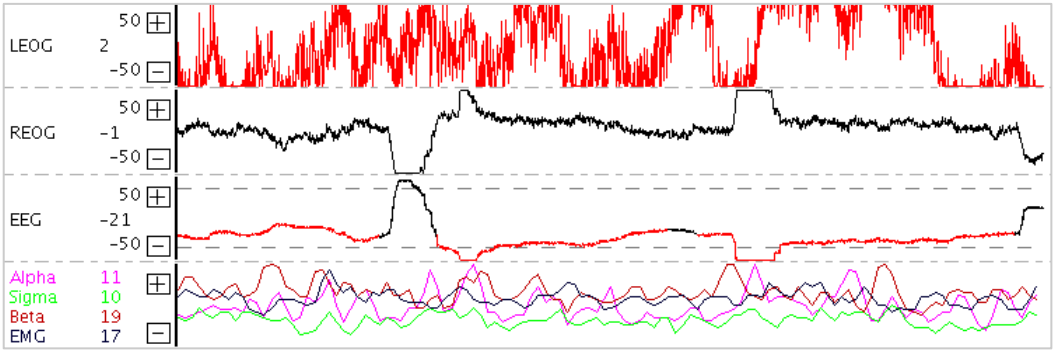

Figure 14. Noisy EEG Data from the X4 Sleep Profiler

Chapter 4: Instrumentation Setup

Biosensors validated in the previous chapter can be used individually or collectively in float research. The following subsections describe protocols for both use cases and examine the validity of comparing data from separate devices to identify common events.

4.1 Overall Setup

As described before, the Kinect observes participants from above the float tanks. It can either be mounted to the ceiling of the room or the ceiling of the enclosed tank. The main limitation that dictates the Kinect's placement is its field of view (FOV). If a participant does not fully fit in the FOV, joint points outside the FOV are often displayed with jitter, which leads to false positives when counting joint movements. For this reason, the Kinect must be placed high enough above the float tank to ensure a sufficiently wide FOV.

According to [41], the Kinect's FOV is 43° vertical by 57° horizontal. Since the float tanks are approximately 8 ft. in diameter, the smaller of the two viewing angles requires the Kinect to be placed 10.155 ft. feet above the surface of the water for the FOV to encompass the entire tank and participant. If the Kinect cannot be placed this high, as is the case with the enclosed tank, then joint points out of view must be estimated and filtered in order to remove noise and jitter. Another option is to switch the Kinect to

seated mode. This mode tracks only upper body joints and reduces the required height to 6.446 ft.

The GENEActiv Original accelerometers come with straps so that they can be easily attached to the wrists or ankles. The straps can also be removed so that the device can be attached to other areas of the body such as the chest or hips. As shown in Figure 15, the pins of the device face the ground in order to correctly orient the xyz-directions. The only time this is different is when the accelerometer is placed on the left wrist. In this position, the pins should face upward to help differentiate the left wrist from the right wrist. Any number of GENEActiv accelerometers can be used to track movement and activity, but the level of invasiveness increases with each added device. For this work, one accelerometer is placed on each wrist.

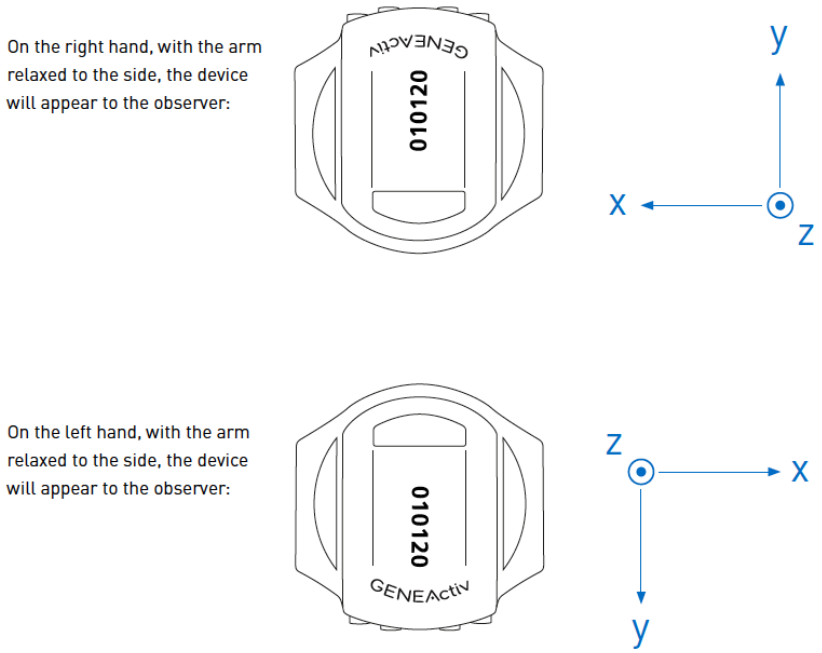

Figure 15. GENEActiv Accelerometer Placement [42]

The packaging of the BioPatch instructs users to place the device on the chest above the sternum. Although the BioPatch successfully records ECG in other positions, it usually fails to capture a valid breathing waveform. Placing the device above the sternum ensures accurate collection of ECG and breathing waveforms while also preventing the device from being submerged in water.

To validate the recommended placement, 21 subjects wore the device above the sternum for 2 90-minute float sessions each. One session was in the enclosed tank while the other was in a reclining chair. As described earlier, the BioPatch records a heart rate confidence value to characterize the signal-to-noise ratio of the ECG signal. It also produces a breathing rate confidence value, and the averages of these values throughout

the float session are depicted in Figure 16 and Figure 17. As can be seen, the average heart rate and breathing rate confidence values are always higher than 80, except when the subjects are initially entering the tank or getting seated in the recliner. The BioPatch manual states that heart rate can be accurately calculated as long as the confidence value is above 20 [43], and this threshold is maintained for all float sessions except four. In these sessions, there was no major difference between floating in the enclosed tank and sitting in the recliner, which suggested that the float environment was not the source of the noise. Even in these cases, the ECG signal was clean enough to visually identify key components of the waveforms. These results verified that placing the BioPatch above the sternum ensures successful collection of ECG and breathing waveforms.

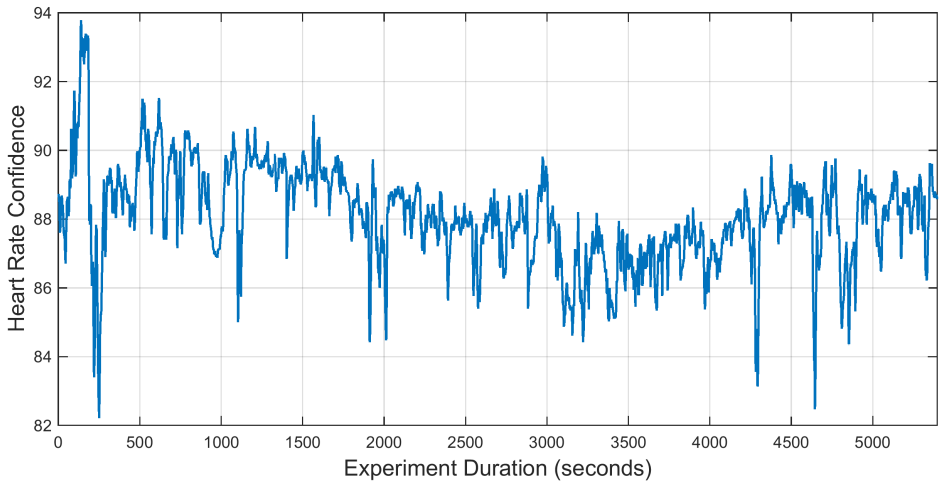

Figure 16. Average Heart Rate Confidence for 42 Float Sessions

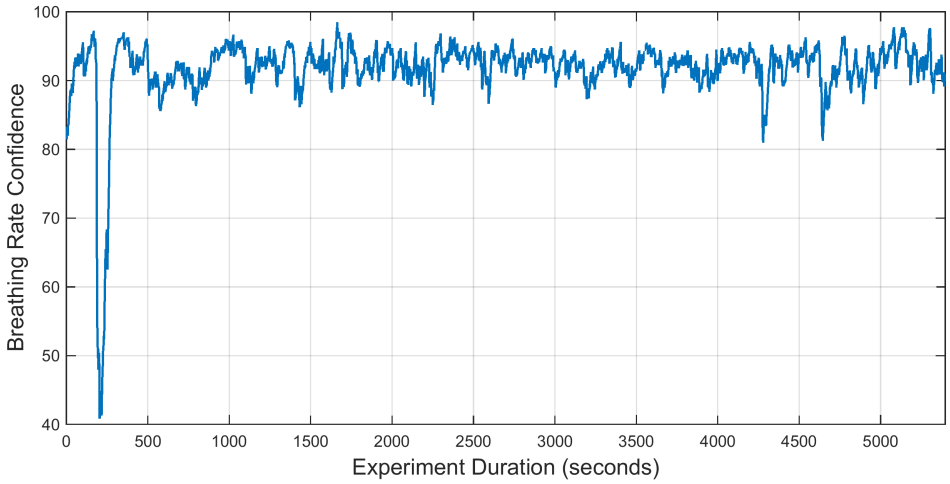

Figure 17. Average Breathing Rate Confidence for 42 Float Sessions

As recommended by most physicians and the provided user manual [44], the QardioArm blood pressure monitor is placed on the left arm at least an inch above the elbow. This position guarantees that the device is at the same height as the heart, especially when participants are floating in a supine position. Using the device on the left arm only for all participants removes the need to correct for lateral differences and simplifies data analysis.

The BrainStation is always placed on the forehead. It is positioned as close to the eyebrows as possible to avoid contact with the salt solution in the tanks. This is the intended placement and allows collection of frontal EEG.

These devices can be used separately to study one variable at a time or collectively to examine common effects and relationships between variables. Regardless of the use case, the placement of each device is the same. The main factor to consider when using

multiple devices is whether or not the participant is being removed from the float experience. In an experiment involving 21 subjects floating with the Kinect, GENEActiv accelerometers, and Biopatch, most people reported a decreased sense of relaxation compared to floating without any devices. For this reason, it is suggested to determine the level of invasiveness of devices before using them in a study. The overall setup of the biosensors is displayed in Figure 18.

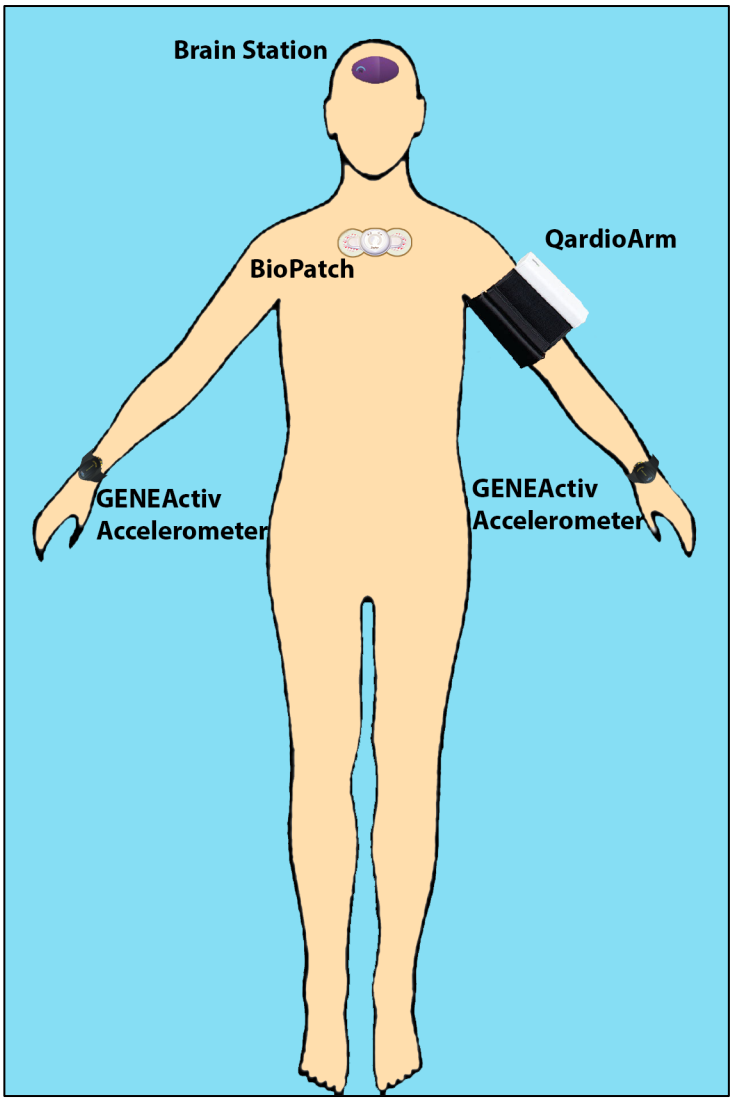

Figure 18. Overall Setup of Biosensors

4.2 Time Sync Evaluation

The following subsections detail the time synchronization protocols employed when using multiple devices simultaneously. For devices that require greater precision in timing, more advanced methods are developed and tested.

4.2.1 Time Synchronization Protocol

Table 3 contains the physiological variables and waveforms examined in this study along with the frequencies at which they are sampled. As can be seen, the fast-changing waveforms are sampled at higher frequencies and then used to calculate metrics reported at lower frequencies. These slower-changing metrics do not usually require timing precision to the millisecond. For instance, there is no need to determine the exact millisecond that arm movement began and match it to the nearest R-peak in an ECG waveform. For these slower-changing variables, a simple protocol was developed to ensure at least one-second precision of time stamps among devices.

Table 3. Biosensor Variables and their Frequencies

Device	Measure	Frequency
Kinect	Joint Positions	30 FPS
GENEActiv Accelerometer	Acceleration	100 Hz
	Sum of Vector Magnitudes	1 Hz
QardioArm	Blood Pressure	> 1 per Minute
BrainStation	EEG	250 Hz
BioPatch	ECG	250 or 1000 Hz
	Breathing Waveform	25 Hz
	Acceleration	100 Hz
	Heart Rate	1 Hz
	Heart Rate Variability	1 Hz
	Heart Rate Confidence	1 Hz
	Breathing Rate	1 Hz
	Breathing Rate Confidence	1 Hz
	Activity	1 Hz
	Posture	1 Hz

The computers used in this thesis are connected to a Network Time Protocol (NTP) server, and the networked computers automatically synchronize their clocks to match the time of the NTP server. The BioPatch and GENEActiv accelerometers sync their clocks to whichever computer they are connected to, so this protocol requires that both devices be synchronized to the same computer prior to each float session. Skeleton joint points from the Kinect are time stamped with the time of the local computer, so it is mandatory that the Kinect be connected to the same computer that is used to synchronize the BioPatch and GENEActiv devices. The QardioArm and BrainStation timestamp each of their measurements using the smart phone or tablet to which they are connected, and these clocks should closely match the NTP server since they also sync to

an NTP server via WiFi or to a cellular tower. Syncing each clock to an NTP server or cellular tower in this way ensures similar timestamps between the BioPatch, QardioArm, BrainStation, GENEActiv accelerometers, and Kinect.

To illustrate the usefulness of this protocol, 15 subjects participated in 2 float sessions each while wearing the BioPatch and GENEActiv accelerometers as stated in Chapter 3. In this experiment, participants were asked to stand for a three-minute baseline test before entering the float tank or sitting in the recliner. Throughout the remainder of the experiment, participants were led through various heartbeat counting tasks and asked to grab and discard an item used for a few of the tasks until the end of the test. The timings of these events are marked on the graphs of Figure 19.

The lower graph of Figure 19 reveals that the GENEActiv accelerometers show significant amounts of acceleration at the times when participants transition from standing to lying down and when they are required to grab or discard the heartbeat-counting object. Comparing this data to the upper graph of Figure 19 shows that quick heart rate changes typically induced by movement or changes of position occur at the same moments when the accelerometers show significant movement. From this it is apparent that the timestamps of the accelerometers are sufficiently synchronized with those of the BioPatch and that comparisons can be made between the time courses of the two biosensors.

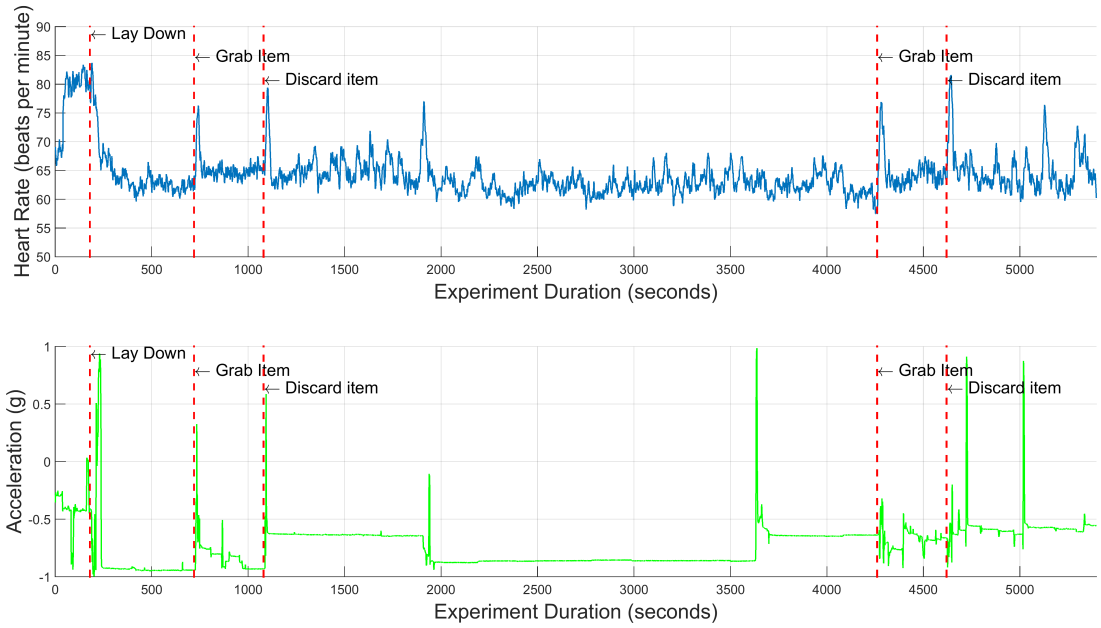

Figure 19. Comparing Average Heart Rate with One Subject's Accelerometer Data

Additionally, the timestamps of the BioPatch's posture data can be used to determine when a participant lays down in the float tank or sits in the chair. Figure 20 is a plot of the posture of two participants, one in each scenario. The data reveals that the participant getting into the float tank required more time to transition to a supine position than the participant that sat in the recliner, which makes sense logically. The timestamps can be analyzed to determine when each participant actually began his or her float session.

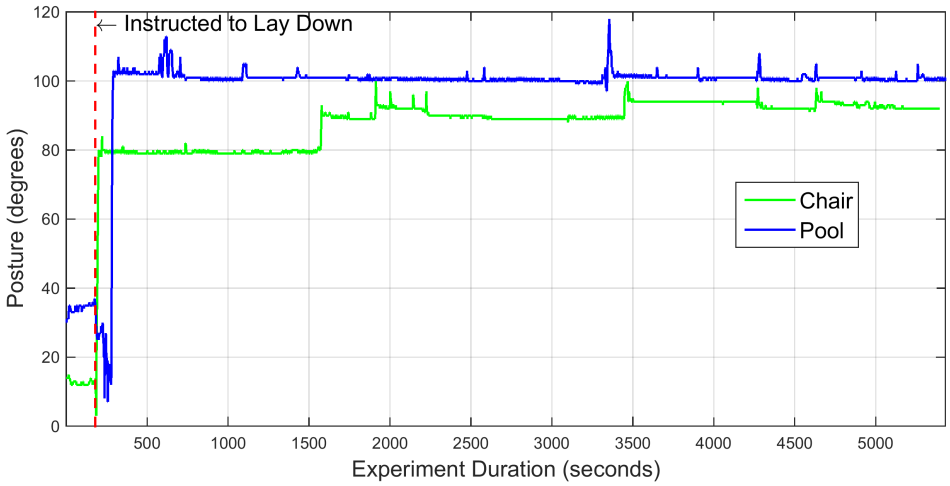

Figure 20. One Subject's Posture Changes during Two Float Sessions

Many of the devices mark data points with millisecond time stamps, but this can be misleading. The real-time clocks of these devices only keep track of time to the second, and milliseconds are counted up from zero each time a device is turned on. The implication is that timestamps can contain an inherent difference between their time and the computer's time. This difference can vary anywhere from 1 to 999ms as explained in the next subsection. Since most variables do not change drastically from second to second, the effect of this difference is small. If devices require precision greater than one second, more complex synchronization methods must be devised.

4.2.2 RR-Interval-Based Synchronization of ECG Waveforms

Float research sometimes examines reaction times and biofeedback by comparing variables from separate devices. One such experiment studies subjects' ability to sense their own heartbeat and requires a response each time a heartbeat is felt. In order to

calculate reaction times between the R-peak of the heartbeat and the response of the subject, millisecond time precision is required.

To determine whether or not this requirement could be met by the previously described protocol, ECG waveforms were simultaneously recorded using the BioPatch and a BIOPAC ECG device. The BIOPAC system can be configured to record data at various sampling rates and serves as an industry leader for accurately collecting physiological data. After collecting and plotting multiple recordings, it was found that the waveforms of the two devices never align in time as can be seen in Figure 21. This held true for 10 recordings, and in each one, the distance between corresponding R-peaks was different. To determine if the variable misalignment was at least constant within a test, each R-peak from the BioPatch waveform was paired to the closest R-peak of the BIOPAC waveform, and the distance in samples between each pair was calculated. The standard deviation of each test's distances was always greater than 50ms. This revealed that the time synchronization protocol was not sufficient for providing millisecond precision and suggested that the BioPatch clock may have an internal drift. These findings led to a discussion with the manufacturer of the BioPatch, and key details of the BioPatch's real-time clock were discovered.

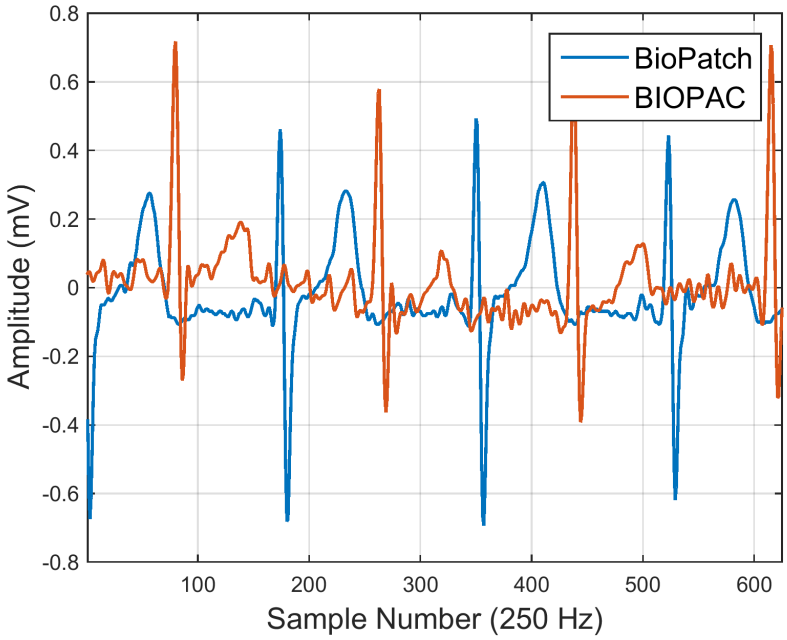

Figure 21. Simultaneously Recorded ECG Waveforms

The real-time clock of the BioPatch is synchronized to a computer anytime it is attached via USB, but it only tracks time to the second. This means that if the local computer time is 12:03:42.347, the clock of the BioPatch will be set to 12:03:42, and the 347 milliseconds will be truncated. This creates an initial constant offset of 347 milliseconds, and this offset is different each time the device is connected to the computer. The offset can vary anywhere between 0 and 999ms based on the local time of the computer when synchronization occurs. Additionally, another offset is introduced when the BioPatch is powered on. Since the real-time clock only keeps time to the second, the BioPatch software begins counting milliseconds starting at zero only when the device is turned on in order to timestamp data points with millisecond resolution. This means that if the device was turned on at 12:05:16.893, the BioPatch clock starts at 12:05:16.000, and the software counts up one millisecond at a time. This creates another

constant offset of 893ms, creating a total offset of 1240ms. As before, the second offset can vary anywhere between 0 and 999ms based on when the BioPatch is powered on, meaning the total offset can vary between 0 and 1998ms. This explains why simultaneous recordings result in signals with variable offsets.

Although the BioPatch maintains a wireless connection via Bluetooth, it is unable to utilize this connection to resynchronize its clock. Since there is no way to sync or probe the BioPatch's clock and determine its time until after the device is turned off and data is downloaded, the offset has to be corrected in post processing. Usually such time synchronization is achieved in the BIOPAC system by injecting a digital signal into the data streams and using the start of the signal as time zero. In the case of the BioPatch and BIOPAC recordings, they already contain a common signal, the ECG waveform, but the morphologies of these two waveforms differ greatly and make it difficult to identify the same heartbeat in each signal. Simply shifting the waveforms left and right to align nearby heartbeats failed to align the signals as illustrated in the plots of Figure 22. After two shifts of the waveforms, the distances between closest R-peaks were calculated by subtracting the locations of the BIOPAC R-peaks from those of the BioPatch R-peaks. For the first shift, the mean difference was -11ms with a standard deviation of 98ms. The second test yielded a mean difference of 10ms and a standard deviation of 67. This reinforced the possibility of a drift existing in the BioPatch's real-time clock.

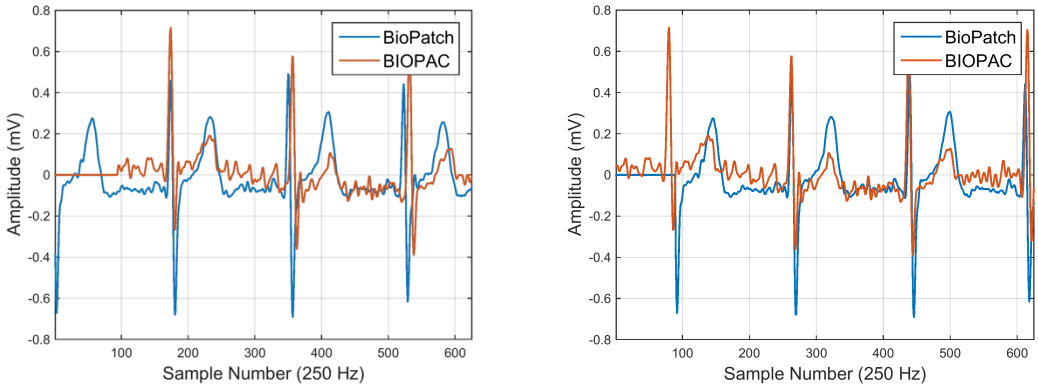

Figure 22. ECG Waveforms Shifted to Align R-peaks

A drift in the real-time clock of the BioPatch would result in inaccurate RR-intervals, which are the distances between consecutive R-peaks in an ECG waveform. To examine this, the RR-intervals of each waveform were plotted, and the results are displayed in Figure 23. The figure reveals that the two RR-interval plots are nearly identical, but one is shifted by a specific number of samples. This verified that the BioPatch was recording without any drift in its real-time clock, and the shift revealed how to correctly align the two waveforms. If the number of samples between corresponding RR-interval plot points is three, this means that the distance between the first and second R-peaks of one waveform are equal to the distance between the fourth and fifth R-peaks of the other waveform. Thus, the first R-peak of the first waveform corresponds to the fourth R-peak of the second waveform. Due to the variation that exists in the offset of the BioPatch's clock, the peaks that correspond to each other can vary for each recording. The RR-interval plots provide information about which heartbeats should be matched to align both waveforms.

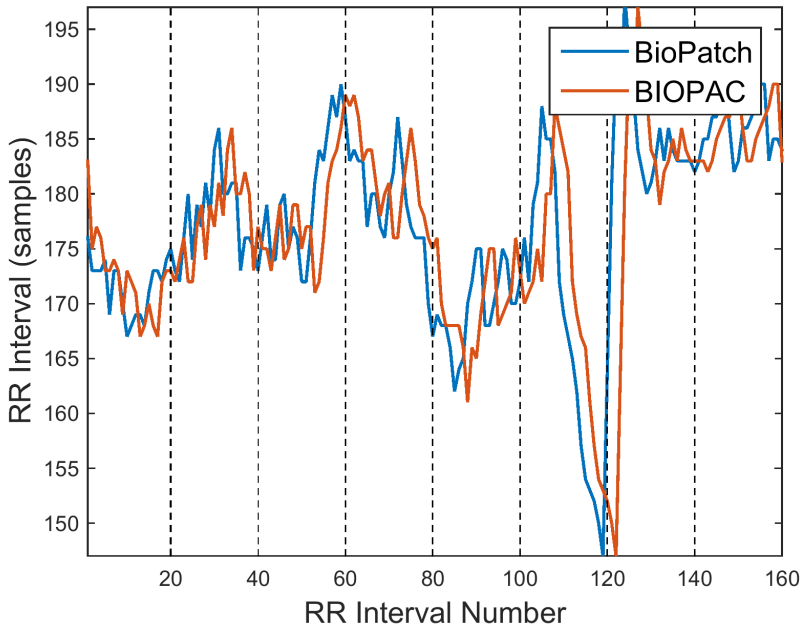

Figure 23. RR-interval Plots

Using this information, a simple method to calculate the shift between RR-interval plots was developed and used to determine the number of samples to shift one waveform to align it with the other. For simultaneously recorded BioPatch and BIOPAC ECG waveforms, the RR-intervals of each signal are plotted together, and the graph is split into windows of 20 samples each as shown in Figure 23. The max value of each plot in each window is found, and difference between max points is calculated. Taking the mode of the differences of each window yields the RR-interval plot shift value. Using multiple windows reduces error caused by slight differences in RR-interval values. Once the shift value is determined, it is used to correctly match the R-peaks of one waveform to the R-peaks of the other, and the distance between matched peaks is calculated. The mean distance is the offset of the BioPatch's clock and is used to shift one waveform to align with the other as displayed in Figure 24. For simplicity, the shift

is achieved in this plot by appending the correct number of samples with a value of zero to the beginning of the waveform being shifted. In this way, timestamps of the BioPatch can be corrected and used to accurately calculate response times in float studies involving heartbeat perception.

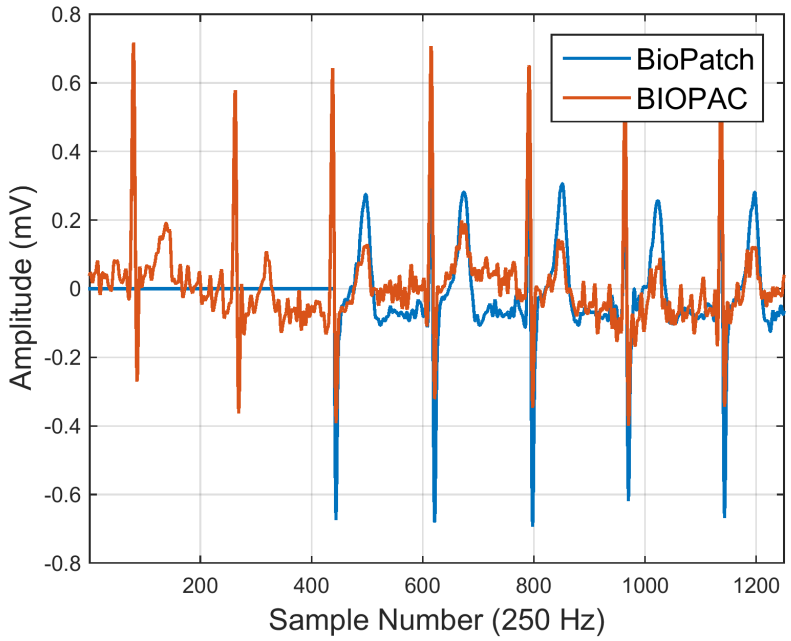

Figure 24. Synchronized Waveforms Using RR-Interval-Based Method

This method was validated in 6 90-minute simultaneous recordings. After shifting the waveforms of each test to align properly, the mean, standard deviation, maximum, and minimum of differences were calculated for corresponding R-peaks, and their values are displayed in Table 4. As can be seen, each shift resulted in a mean difference between corresponding R-peaks of less than 0.3ms with standard deviation below 2ms, which verified the accuracy of the method.

Table 4. Delay Stats for Matched Waveforms

Delay (ms)	**Test 1**	**Test 2**	**Test 3**	**Test 4**	**Test 5**	**Test 6**
Mean	-0.205	0.168	0.123	0.137	0.149	0.271
SD	1.367	1.502	1.374	3.183	1.749	1.985
Max	4	5	6	27	6	56
Min	-4	-5	-5	-136	-7	-9

The drawback of this method is that it requires simultaneous recordings to be obtained before each experiment. This adds to the total experiment time and to the overall analysis process. For these reasons, an additional method was developed and validated by comparing it to the RR-interval-based method.

4.2.3 Parallel-Port-Based Synchronization of ECG Waveforms

As stated in the previous subsection, the BIOPAC system uses a digital signal to synchronize simultaneously collected data. A parallel port produces this digital signal, and a time stamp can be recorded when the signal is injected. This time stamp can be compared to the time stamp of a device that receives the signal to determine the offset of the device's clock. Using the parallel port, a prototype was designed to inject a digital signal into the ECG waveform of the BioPatch.

The prototype depicted in Figure 25 consists of ECG electrodes, wire connectors, and the parallel port and its connector. The wire connectors run from pins of the parallel

port connector to the ECG electrodes to inject the digital signal into the BioPatch when it is connected to the electrodes. The computer saves the time at which the signal is injected, and this time stamp is compared to the time stamp of the BioPatch to determine the offset.

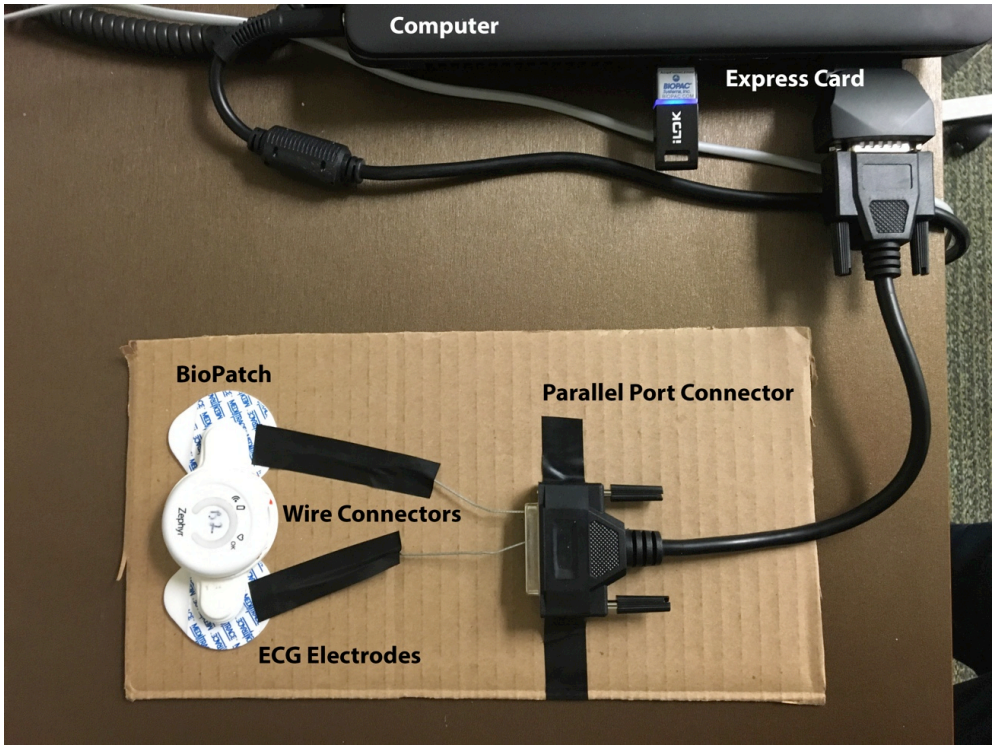

Figure 25. Parallel Port Prototype for Synchronization

This method was tested by powering on the BioPatch device, injecting the 5V digital signal into its ECG waveform, and then recording ECG simultaneously with the BioPatch and BIOPAC devices. After data collection, the portion of the BioPatch ECG waveform containing the digital signal was used to determine the offset. As Figure 26 reveals, injection of the digital signal drives the ECG waveform to a max value. The time stamp that matches the sample with this max value was identified and compared to

the time stamp of the digital signal to calculate an offset value of 400ms. The offset was then used to correct the time stamps of the BioPatch's ECG waveform.

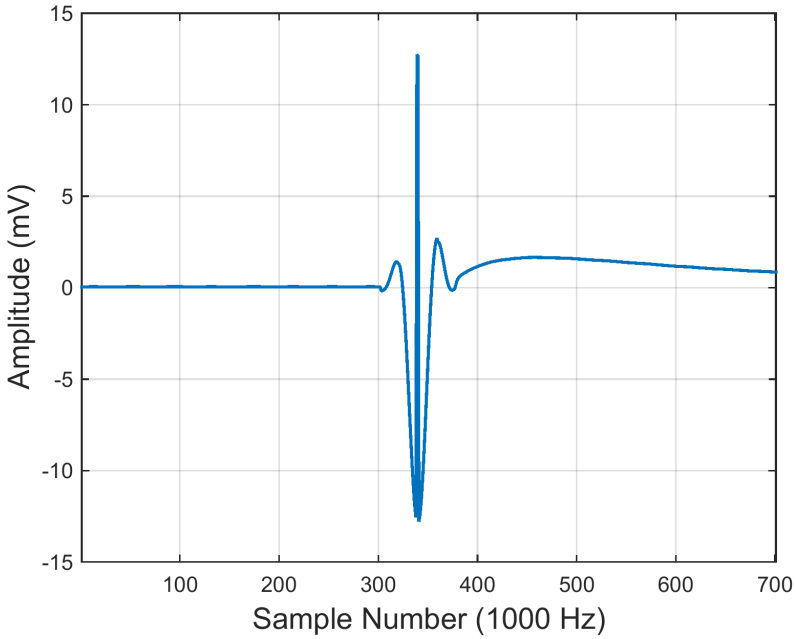

Figure 26. ECG Waveform with Digital Signal

The RR-interval-based method was also used for this test and resulted in an offset time of 398ms. Using the offsets, the waveforms were plotted for each method, and distances between corresponding R-peaks were calculated as before. Figure 27 depicts the synchronized waveforms. The mean difference in R-peaks was 0.307ms with a standard deviation of 0.930ms for the parallel-port-based method as compared to a mean of 0.284ms with standard deviation of 0.914ms for the RR-interval-based method. Although the parallel-port-based method yields slightly less accurate results, it ultimately provides a way to synchronize the BioPatch clock without requiring

simultaneous ECG recordings. Either of these methods can be used to synchronize the BioPatch's clock as the researcher sees fit.

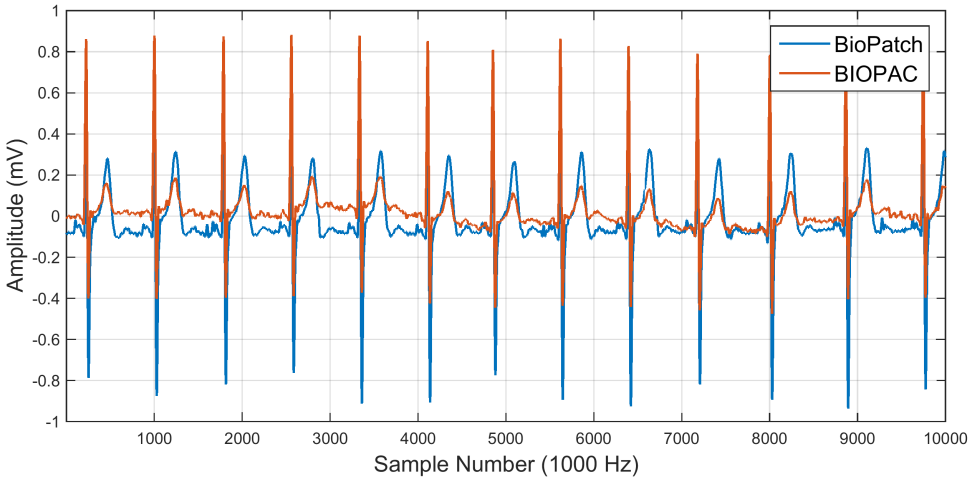

Figure 27. Synchronized Waveforms Using Parallel-Port-Based Method

Chapter 5: Using a Neural Network to Calculate Cardiac Metrics

Cardiac metrics such as heart rate and heart rate variability (HRV) often provide information about the circulatory, respiratory, and nervous systems [29], [45]. Unfortunately, the BioPatch's cardiac algorithms lose some of this data. These algorithms filter and smooth the ECG signal and calculate variables using methods that fail to characterize respiratory-linked variability and cardiac vagal control. In order to regain this information, this chapter develops an artificial neural network (ANN) to automatically detect the R-peaks in raw ECG signals. These R-peaks are then used to illustrate how researchers can calculate heart rate and HRV using methods that yield the most useful information for float research.

5.1 A Neural Network for Automatic Detection of R-peaks

ECG signals represent the electrical activity of the heart and contain a repeating P-wave, QRS complex, and T-wave as shown in Figure 28. The peak of the QRS complex is known as the R-peak and is used to calculate heart rate, HRV, and RR intervals. The shape and amplitude of each wave or complex in the ECG signal depends on electrode placement, patient physiology, and noise. Variation in these parameters makes automatic R-peak detection difficult.

Various algorithms have been developed to automatically identify cardiac events. In [46], the authors build upon common thresholding techniques to create an adaptive

double threshold method for R-peak detection in real time, and the authors of [47] use the Pan-Tompkins algorithm, which also employs multiple thresholds, combined with a wavelet transform to increase detection accuracy. Since these methods rely heavily on amplitude thresholds, they often perform poorly in the presence of noise and artifacts.

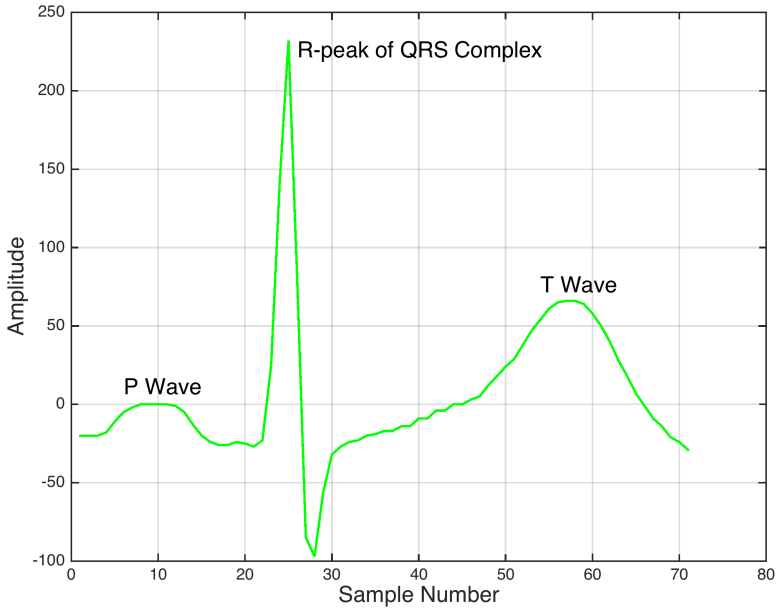

Figure 28. Components of an ECG Signal

Other studies have shown that neural networks deal well with noise and baseline drift. Szilagyi compared neural-network-based adaptive filtering and the wavelet transform to detect R-peaks [48]. The wavelet transform magnifies QRS complexes at finer scales, while the neural network removes noise via whitening. Both methods use a thresholding technique to find R-peaks in the final signal, and it was shown that neural networks usually outperform wavelet-based methods. A more complex adaptive filter is presented in [49]. This method uses two neural networks; the first acts as an adaptive filter to

whiten the ECG signal, and the second is used in a matched filter that outputs a signal with well-defined QRS complexes. Thresholding is performed on this final signal to detect R-peaks. This type of filtering requires a large amount of training data.

A simpler neural network presented in [50] is a two-layer tan-sigmoid/linear network. It uses amplitude, differentiation, duration, RR interval, a zero-crossing flag, and a first-element flag as inputs and updates weights via back propagation. It outputs a 1 for an R-peak and a 0 for not an R-peak instead of filtering the ECG signal. It is applied in real-time and provides an accurate method of detecting R-peaks.

Since the literature revealed neural networks to be effective in dealing with nonlinear background noise and baseline drift, this study designed one to automatically detect R-peaks. The following subsections detail the neural network's design and the results of testing it with ECG signals collected during float experiments.

5.1.1 Network Design

Figure 29 illustrates the structure of the designed neural network. The hidden layer uses a tan-sigmoid function to model nonlinear data, while the output layer is linear. There are 4 inputs to the system and 9 hidden neurons. The number of hidden neurons was determined using the 2m + 1 rule, where m is the number of normalized inputs when the network has only one hidden layer [51].

The inputs of the network are amplitude, RR interval, duration above a threshold, and a first-element flag. The network in [50] has two additional inputs, differentiation and a zero-crossing flag. The differentiation did not seem to contribute much to the network's ability to distinguish between peaks in this work, and using the network in post-processing removed the need to segment the ECG signal and check if end points were zero-crossing points. Peaks are provided to the network using a generic peak-detection algorithm that finds max points preceded by points below a specified threshold [52]. Additionally, there is a bias node in the input and hidden layers with constant values of one.

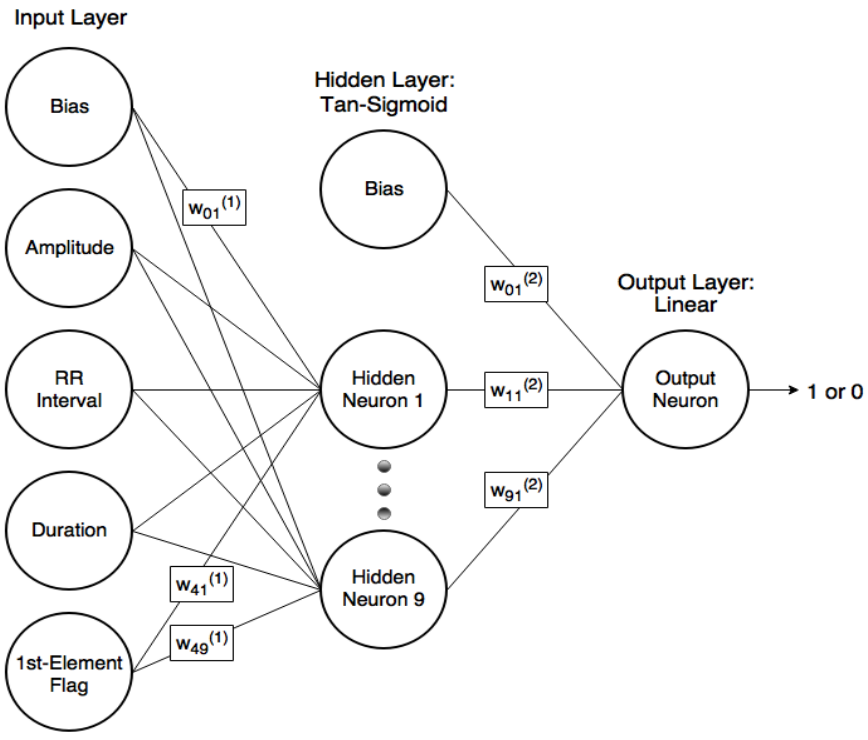

Figure 29. Neural Network Structure

Each input and bias of a network layer is connected to each neuron of the next layer, and each connection has a corresponding weight. The notation $w_{ij}^{(n)}$ represents the weight in layer *n* of input *i* to neuron *j* of the next layer. These weights are updated via standard back-propagation with an added momentum variable to help avoid local minimums. The output neuron simply sums the weighted inputs of the previous layer, and a threshold of 0.5 is used to output a 1 for R-peaks and a 0 for all other points.

To obtain ECG data to train and test the network, 21 subjects spent 1 session in the float tank and another in a reclining chair while wearing the BioPatch. The sessions were each 90 minutes long, but 40 minutes in the middle were allotted as a rest period with no activity. These 40-minute periods were used to collect data to train and test the neural net. From the resulting 42 ECG signals, 10 were chosen for training, 10 for validation, and 15 for testing. Signals with greater amounts of noise and baseline drift were placed in the testing set to determine the limitations of the neural network. For each of the ECG signals, the first 10 seconds were used for training and validation. Initial testing also used the first 10 seconds of the signals, but later tests used the full 40 minutes to test the network's ability to work with data recorded for longer periods of time.

5.1.2 Training and Validation

The network was trained using 10 10-second signals recorded while participants were in the float tank or reclining chair. Each point in the signals was manually labeled as either

a 1 for an R-peak or a 0 for not an R-peak. Using the peak-detection algorithm with a low threshold value, peaks were detected, and then their amplitude, RR interval, duration, and first-element flag were determined. The RR interval is defined as the interval from the current peak to the last R-peak. The duration is calculated as the distance between the points to the left and right of the current peak that are half the peak's amplitude. The first-element flag is a 1 if the detected peak is the first R-peak or any peak that occurs before the first R-peak and a 0 otherwise.

After all the inputs are extracted for each detected peak in each signal, they are normalized. This prevents large values from saturating the neurons. There were approximately 629 example peaks, and the network was given the inputs and target output of each for training. The network randomly selects examples and updates its weights using back-propagation of the network error. After training the network for 800 epochs, the weights that achieved the lowest mean squared error (MSE) were saved and used with the validation and test datasets.

A validation dataset of 10 additional 10-second signals was used to determine what threshold value to use with the peak-detection function during testing. This function takes in a threshold value as input and returns peaks that have a max value preceded by a value lower than the threshold. The threshold was set to a very low value to obtain many peaks for training data, but its value should be tested to optimize accuracy during testing. Using a validation dataset to select the threshold serves this need while preventing contamination of the test dataset. To measure the results of each threshold

value, accuracy was defined in terms of sensitivity and positive predictivity. These measures prevent false positives from resulting in traditional accuracy scores greater than 100%. Sensitivity and positive predictivity are defined as

$$sensitivity = \frac{TP}{TP+FN} \tag{5.1}$$

and

$$positive\ predictivity = \frac{TP}{TP+FP}, \tag{5.2}$$

where TP is the number of true positives, FN is the number of false negatives, and FP is the number of false positives.

The threshold was varied from 0.1% to 100% of the max amplitude of the signal in increments of 0.1%, and the average sensitivity and positive predictivity were calculated for each threshold. As shown in Figure 30, both the sensitivity and positive predictivity have max values from threshold values of 5% to 10%. At about 15%, both values drop and plateau until 75% for sensitivity and 87% for predictivity, and then they fall rapidly with further increases in the threshold value. The high accuracy at such low threshold values is most likely do to the fact that many of the BioPatch ECG waveforms contain large T-waves and very small R-peaks. To ensure detection of these low-amplitude R-peaks, the threshold was set to 7.5% of the maximum amplitude for the test dataset. This low threshold also ensures that the neural network's ability to distinguish between types of peaks will be tested instead of relying only on the peak-detection function.

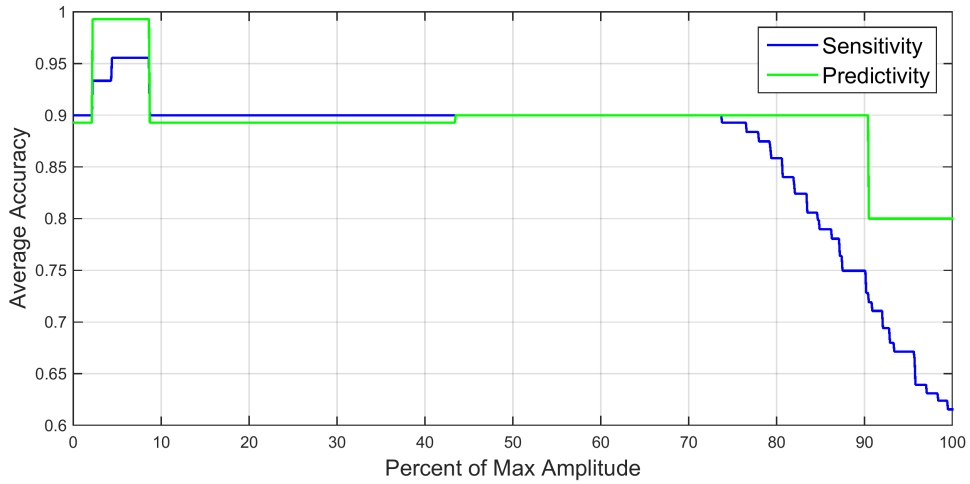

Figure 30. Validation Results of Neural Network

5.1.3 Test Method and Results

The neural network was first tested in 15 experiments, each with a different 10-second signal. Each of the signals contained varying amounts of noise and artifacts and presented different challenges for detection. Figure 31 illustrates the method used for testing new signals.

First, the algorithm loads an ECG signal and determines its max amplitude. Using 7.5% of the max amplitude as a threshold, the peak-detection algorithm identifies peaks in the ECG signal. For each detected peak, the input features are calculated and saved. Initially, only the first detected peak has a 1 for the first-element flag feature, and the RR interval of each peak is the distance between it and the previous peak. For the first peak, the RR interval is simply the distance from the peak to the first point in the signal.

All of the input features are normalized using the mean and standard deviation of the training data, and then the first peak and its features are given to the neural network.

The neural network then uses the saved weights from training to determine whether the peak is an R-peak or not. If the first peak is not an R-peak, the first-element flag of the next peak is changed to a 1. This is repeated until the first R-peak is found. When an R-peak is successfully found, the RR interval of the next peak is updated to reflect its distance from this R-peak. This ensures that accurate RR intervals are calculated. Each time an input is changed, it is normalized before being given to the network. This process is repeated until there are no more detected peaks in a signal. After the last peak has been classified, the sensitivity and positive predictivity of the experiment is calculated, and then the next signal is loaded. Once all the signals have been tested, the algorithm is terminated.

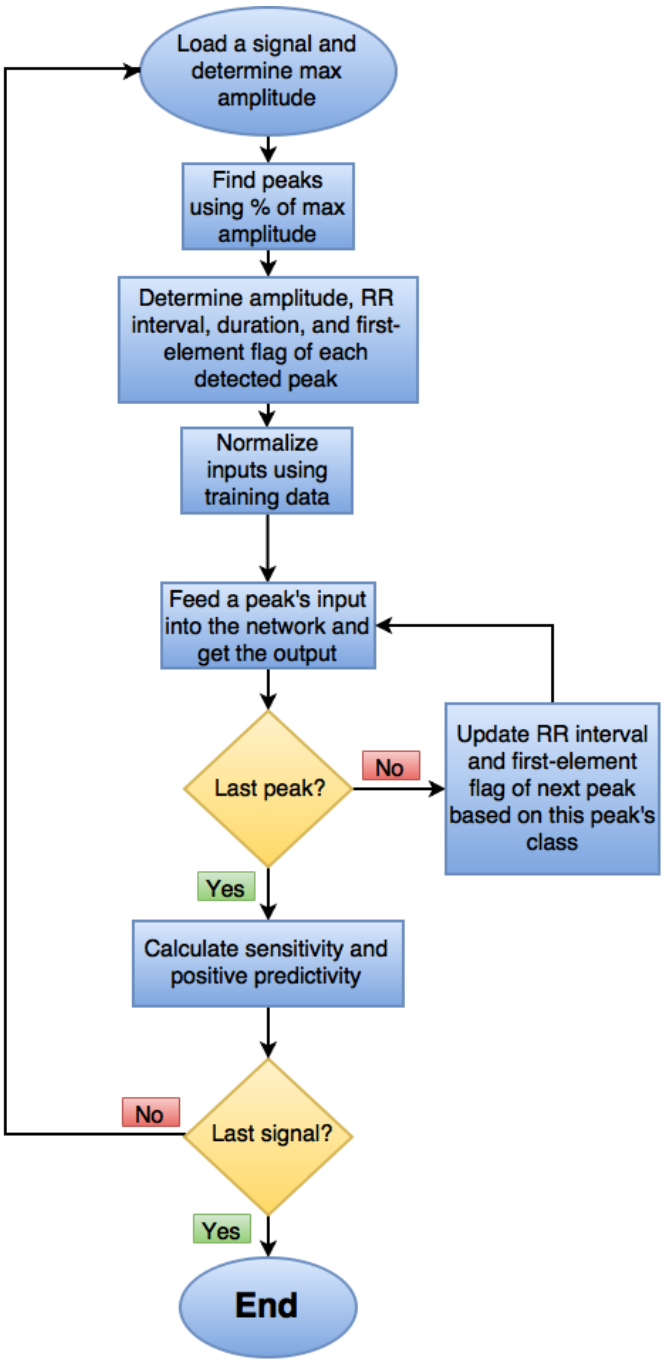

Figure 31. Neural Network Flowchart

The average sensitivity and positive predictivity were 67.0% and 82.8%, respectively, and the results for each of the 15 experiments are displayed in Table 5. The results reveal that the neural network is very effective with certain signals while ineffective

with others. When the R-peaks are dominant, as in Figure 32, the network easily detects them. With significant baseline drift, the network missed an R-peak but was able to recover as seen in Figure 33. Figure 34 illustrates that when the R-peak is very low in amplitude and the T-wave resembles the R-peak, the network confuses each T-wave for an R-peak. Arguably, these can still be used to calculate accurate heart rates and HRV. In the worst case, the R-peak is low and the T-wave does not resemble an R-peak. This results in the network not detecting any R-peaks at all as shown in Figure 35. These results imply that the current network is best suited for cleaner ECG signals and can handle moderate noise and baseline drift. With additional training data, the network can be applied to more signals with greater variety and noise.

Table 5. Accuracy of Neural Network

Experiment Number	Number of R-Peaks	Sensitivity	Positive Predictivity
1	10	100%	50%
2	14	85.7%	100%
3	14	85.7%	100%
4	11	9.1%	100%
5	16	0%	0%
6	12	100%	100%
7	13	92.3%	92.3%
8	12	100%	100%
9	11	45.5%	100%
10	11	0%	0%
11	13	100%	100%
12	13	76.9%	100%
13	12	100%	100%
14	11	100%	100%
15	11	100%	100%

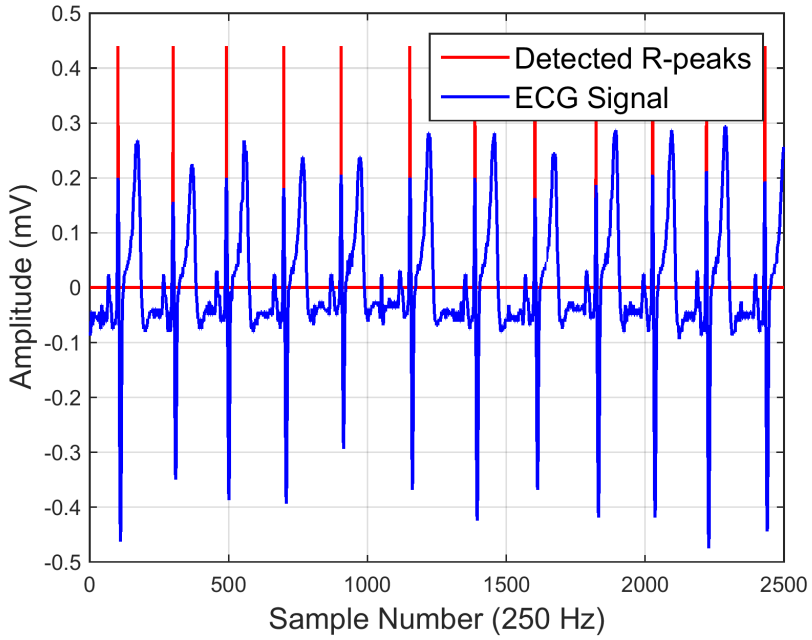

Figure 32. Clean ECG in Experiment 8

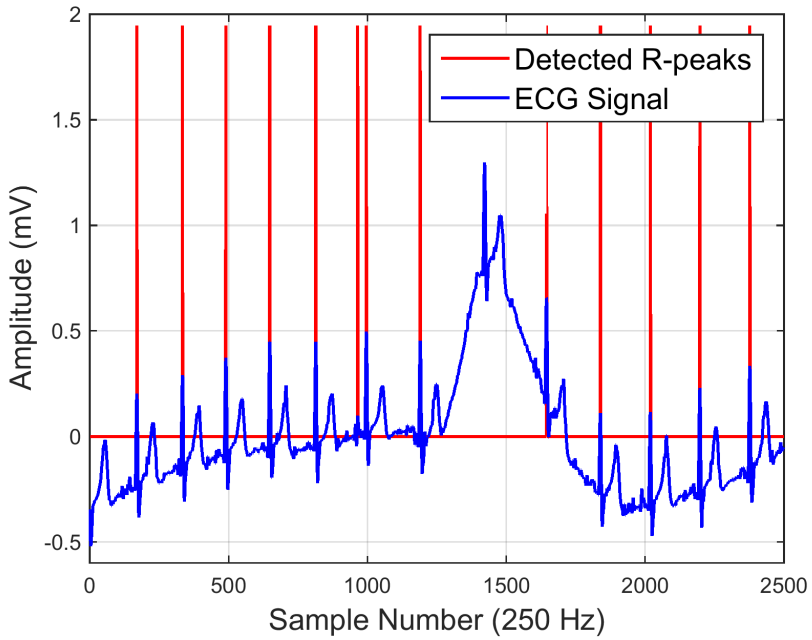

Figure 33. Baseline Drift in Experiment 7

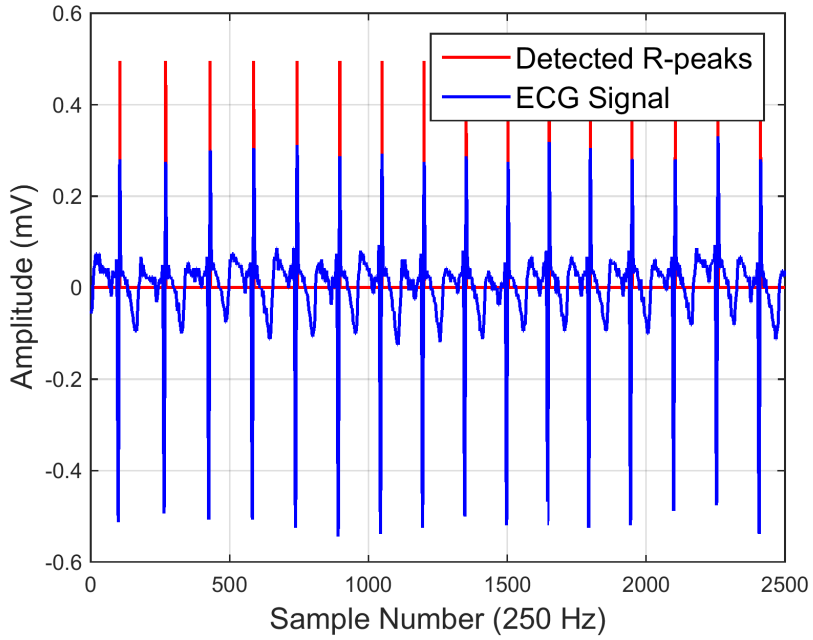

Figure 34. T-wave Confusion in Experiment 5

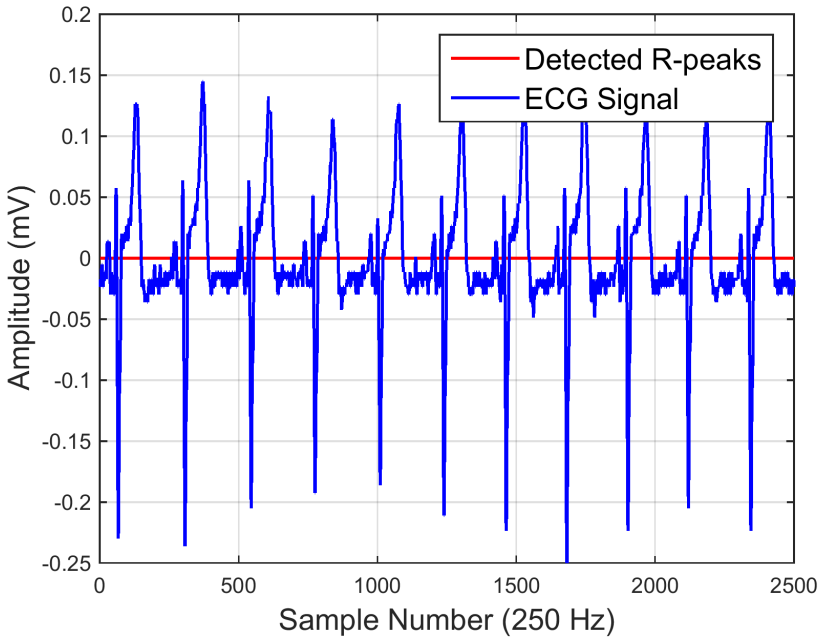

Figure 35. No Detections in Experiment 10

Since the ultimate goal of the network is to detect R-peaks for the calculation of heart rate and HRV from ECG signals recorded during float sessions, the network was tested on 4 of the 40-minute signals. One of these signals was obtained from the training set, two from the validation set, and one from the testing set. This tested the network's ability to work with both familiar and unfamiliar data for longer periods of time.

The results of testing these four signals are displayed in Table 6. As can be seen, there are no more than 6 missed detections out of more than 2100 peaks. One of the signals contained significant baseline drift, which resulted in 45 false detections. Since heart rate and HRV values are usually averaged over large windows containing many peaks, these missed and false detections should have minor effects on the calculated cardiac metrics. The next section uses these detected R-peaks to determine such metrics and proves that the network's error has little effect on the end results.

Table 6. Results of Testing 40-minute Signals

Experiment Number	**Number of Peaks**	**Missed Detections**	**False Detections**
1	3052	0	2
2	2999	1	10
3	2189	1	2
4	2318	6	45

5.2 Calculation of Cardiac Metrics

The BioPatch algorithms use unknown smoothing and filtering techniques before calculating heart rate and HRV. This often removes variability and other information. Using the neural network presented in the previous section, R-peaks can be detected and used to calculate cardiac metrics without the loss of data. This provides full access to the data collected in float research.

5.2.1 Heart Rate

According to the BioPatch's log description manual, ECG is filtered and smoothed to account for missed R-peak detections, and heart rate is calculated using a moving window of 15 seconds [43]. These processes yield heart rate values resembling average heart rate and suppress variability. Since it is more common to calculate heart rate on a beat-by-beat basis, R-peaks detected by the neural network can be used to do so without losing information via filtering.

Using the 40-minute signal from experiment 1, the heart rate was calculated for each R-peak by dividing the number of samples in one second by the current peak's RR interval. The results are displayed in Figure 36. The neural network's two false positives result in the two extreme heart rate values shown in the end of the plot, but such outliers can be removed. Figure 37 illustrates the heart rate values reported by the BioPatch. The BioPatch plot appears to be a smoothed version of the neural network

plot, reinforcing the fact that information is lost when smoothing and filtering is used. These results demonstrate how the neural network can be used to calculate heart rate without losing data. This provides researchers with full access to the data.

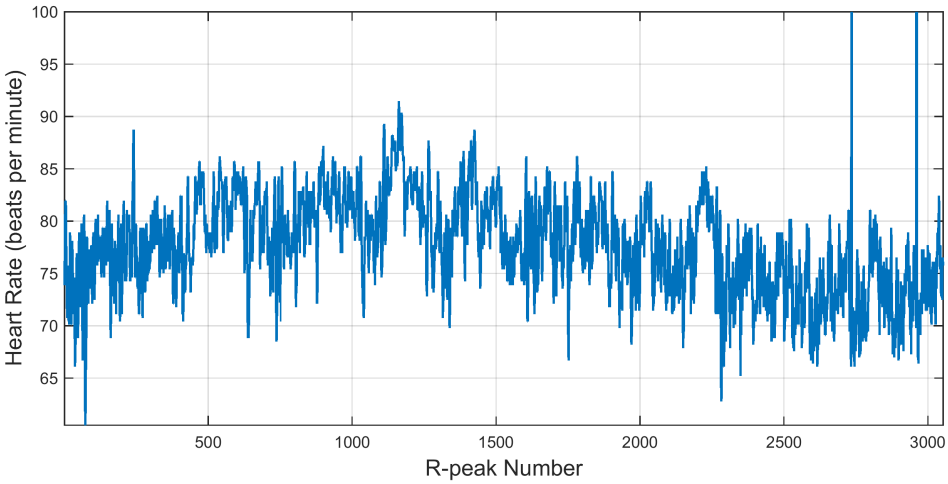

Figure 36. Neural Network Heart Rate for One Float Session

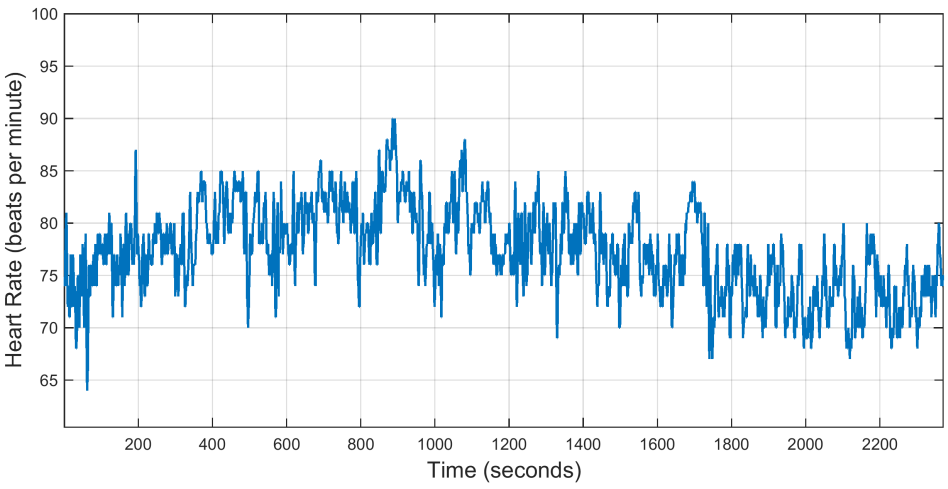

Figure 37. BioPatch Heart Rate for One Float Session

5.2.2 Heart Rate Variability

As with heart rate, the BioPatch reports HRV once per second using a moving window instead of on a beat-by-beat basis. Its algorithm calculates a 300 heartbeat SDNN value, which is the standard deviation of RR intervals. Using the neural network's detected R-peaks, SDNN can be calculated for each peak instead of each second. Like the BioPatch's algorithm, a 300-heartbeat window is used and moved one peak at a time instead of one second at a time. Figures 38 and 39 show the results of calculating SDNN using both methods. As before, the BioPatch yields a smoothed version of the HRV plot. Using the neural network provides more data.

In addition to calculating HRV using the SDNN method, HRV can also be measured using the root mean squared of successive differences (RMSSD). The RMSSD value reflects respiratory-linked changes in the heart. Using detected R-peaks, the RMSSD was calculated, and the results are displayed in Figure 40.

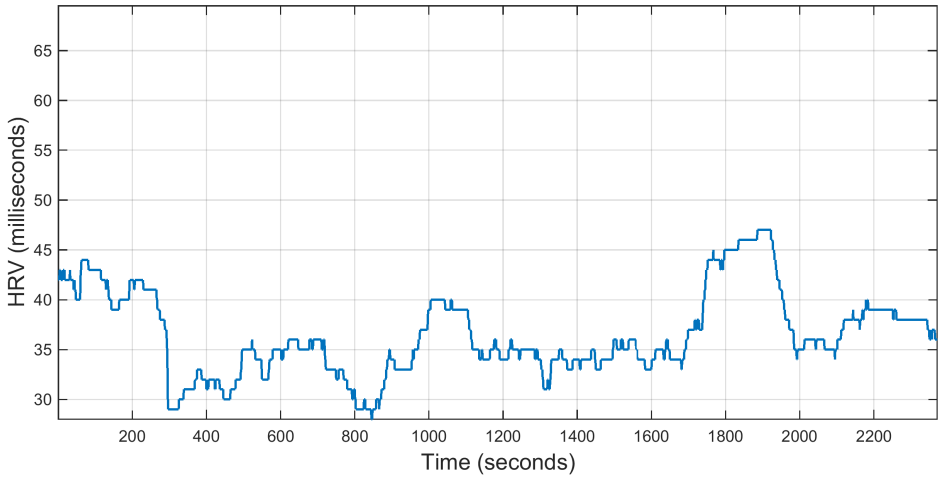

Figure 38. BioPatch SDNN Values for One Float Session

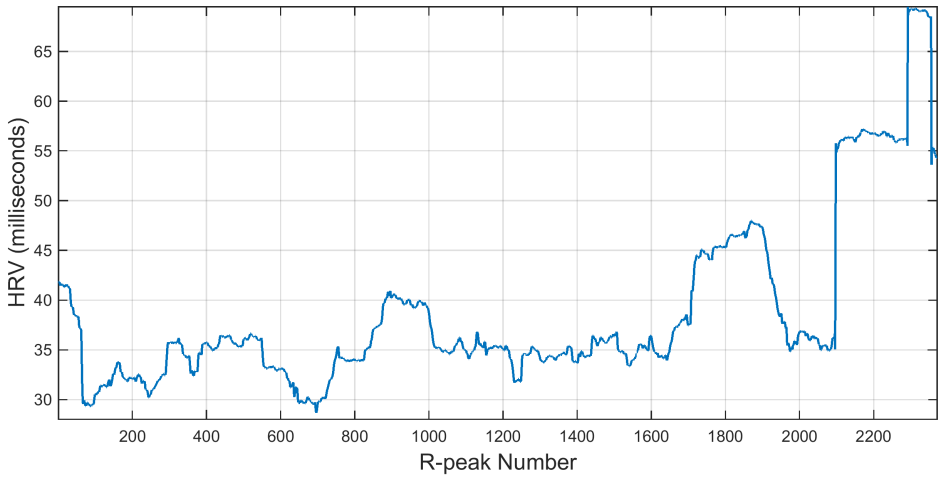

Figure 39. Neural Network SDNN Values for One Float Session

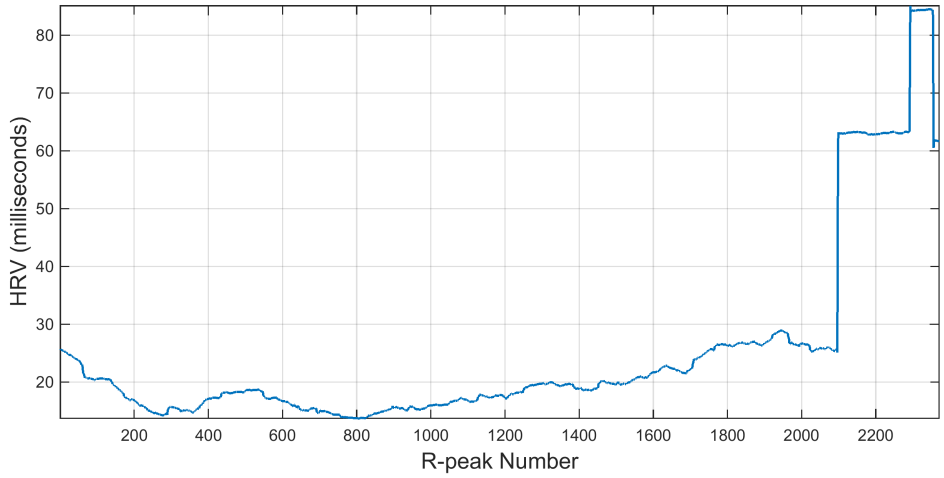

Figure 40. Neural Network RMSSD Values for One Float Session

Although HRV values can be calculated on a second-by-second or beat-by-beat basis, the literature recommends either calculating a single value for the entire recording or calculating a value for each five-minute period [29]. Using the second method, eight SDNN and eight RMSSD values were calculated for the 40-minute recording period and are shown in Table 7.

Table 7. Neural Network's SDNN and RMSSD Values

Bin Number	SDNN (ms)	RMSSD (ms)
1	39.92	24.13
2	36.33	16.77
3	34.11	14.78
4	34.21	15.92
5	36.61	19.39
6	44.19	25.56
7	35.73	25.58
8	52.7	58.55

Once HRV values are calculated for multiple subjects or sessions, various time-domain and frequency-domain analyses can be performed to compare results [29]. The purpose of this study is to demonstrate how the neural net provides complete access to cardiac metrics, so these analyses are not performed here. Future research can utilize the neural net developed in this chapter to analyze the effects that floating has on both heart rate and HRV.

Chapter 6: Measures of Movement – Stillness and Avoidance

For the first time, flotation researchers can study movement throughout float sessions using the Kinect and the accelerometers of the BioPatch and GENEActiv devices. The aim of this chapter is to take the beginning steps in analyzing movement data and develop metrics to characterize it. Using data from the GENEActiv accelerometers, activity thresholds are developed and applied to the BioPatch to provide a measure of stillness throughout float sessions. Additionally, a measure of avoidance behavior is characterized using joint data from the Kinect.

6.1 Stillness

Although three of the selected biosensors are capable of monitoring movement, it is often desirable to use one at a time to reduce overall invasiveness. Since the BioPatch does not require use of a foothold system and is placed in a single location on the body, it is the optimal choice for monitoring stillness. In order to determine whether or not the BioPatch is sufficient for measuring stillness, a receiver operator characteristic (ROC) curve analysis was performed using data recorded with the GENEActiv accelerometers.

To collect data, 11 participants floated for 2 90-minute sessions wearing the BioPatch and a GENEActiv accelerometer on each wrist. One session was in the float tank, while the other was in a reclining chair. After collection, the GENEActiv data was converted into one-second epochs. The BioPatch activity data is reported once per second by

default. Using the timestamps of each device, the 90-minute sections of data were extracted and synchronized in time.

In [26], three thresholds were defined to separate sedentary activities from more than sedentary activities using the GENEActiv accelerometers. Since the aim of this investigation was to measure whether a person is still or not still, similar binary thresholds were desired for the BioPatch. The value used with the GENEActiv devices to characterize movement is the gravity-subtracted sum of vector magnitudes and is calculated as:

$$SVM_{gs} = \sum[(x^2 + y^2 + z^2)^{\frac{1}{2}} - 1g] \quad (6.1)$$

with a unit of g-seconds (g·s). After categorizing activity using oxygen uptake values, the authors of [26] performed an ROC curve analysis with one-minute epochs and chose the thresholds for the left wrist, right wrist, and waist accelerometers to be 217, 386, and 77 g·min, respectively. These values can be divided by 60 seconds to obtain thresholds applicable to 1-second epochs. This results in values of 1.28, 3.62, and 6.43 g·s.

Each of these thresholds was applied to the GENEActiv accelerometer data to create three ROC curves for the BioPatch. For each second of data, the higher of the two values from each GENEActiv accelerometer was compared to the threshold to categorize the second as either still or moving. The resulting data was used to determine the optimal threshold to use for the BioPatch.

The BioPatch reports activity in vector magnitude units (VMU) calculated as:

$$VMU = \sqrt{(x^2 + y^2 + z^2)}, \tag{6.2}$$

where x, y, and z are the averages of the three axial acceleration magnitudes over the previous one second. The reported values ranged from 0 to 1g in the 90-minute floats. ROC curves are produced by incrementing the threshold of a binary classifier and plotting the false positive rate (false positives / (false positives + true negatives)) versus the true positive rate (true positives / (true positives + false negatives)), so the threshold was tested from 0 to 1g in increments of 0.01g. For each threshold, the BioPatch's VMU values were compared to the threshold to categorize each second as still or moving. The results were then compared to the GENEActiv classifications to calculate the number of true positives, false positives, true negatives, and false negatives. These were then used to plot an ROC curve for each of the three tests, and the results are displayed in Figure 41.

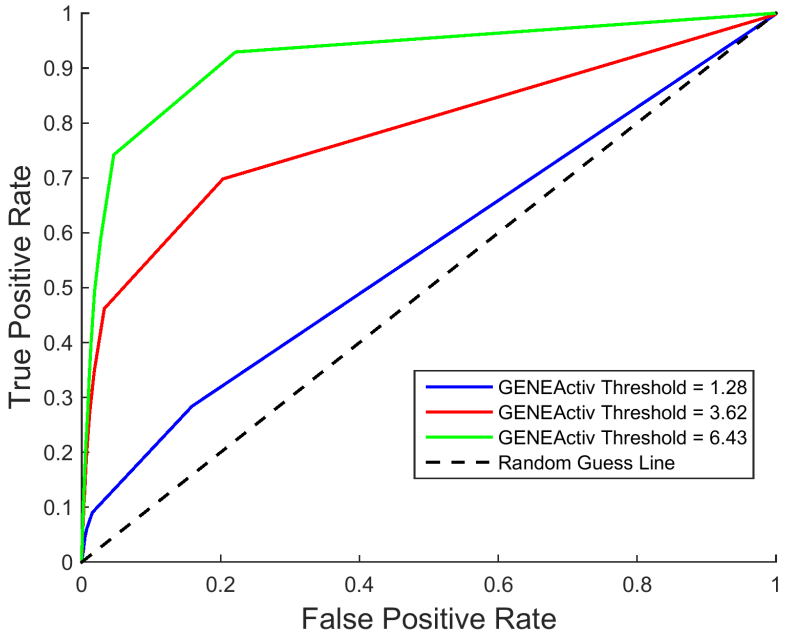

Figure 41. ROC Curves

From the ROC curves of Figure 41, it is apparent that the BioPatch accuracy increases with more lenient thresholds placed on the GENEActiv accelerometers. The area under the curve (AUC) for GENEActiv thresholds of 1.28, 3.62, and 6.43 g·s is 0.567, 0.784, and 0.920, respectively. Optimal thresholds are typically those that maximize the true positive rate while minimizing the false positive rate. For the ROC curve with the maximum AUC, the first false positive rate with a value below 0.10 is 0.046 and yields a true positive rate of 0.742. This occurs at a threshold value of 0.03g. Unfortunately, this threshold results in the BioPatch categorizing 4779 more seconds as moving than do the GENEActiv accelerometers. At a threshold of 0.06g, the BioPatch reports 93.93% of the movement time that the accelerometers do, but the true positive rate drops to 0.400.

As discussed in Chapter 4, the real-time clocks of these devices can have an offset up to 1998ms. This may cause movement seen in one device to appear later in another device, which would result in errors reported during classification. For this reason, it may be more appropriate to select thresholds for the BioPatch that maximize the percent of movement time found by the GENEActiv accelerometers instead of thresholds that correctly label each second of data. Also, since [27] found the GENEActiv cut-points to be somewhat inaccurate, further research is needed to validate the thresholds of both the BioPatch and GENEActiv accelerometers.

To briefly analyze the types of body movement the GENEActiv accelerometers and BioPatch can detect, one subject floated in the float tank wearing all three devices and sustained specific body movements for 1.5 minutes each. For each of the body movements, the middle one minute of data was extracted for analysis. As before, the GENEActiv data was summed to create one-minute epochs, and the BioPatch VMUs were averaged over each minute. Since the values of each device have drastically different ranges, the BioPatch data was scaled for visualization. The values for each device were then plotted together to illustrate the relative levels of activity seen in each device for each body movement. The results are displayed in Figure 42, and Table 8 serves as its key.

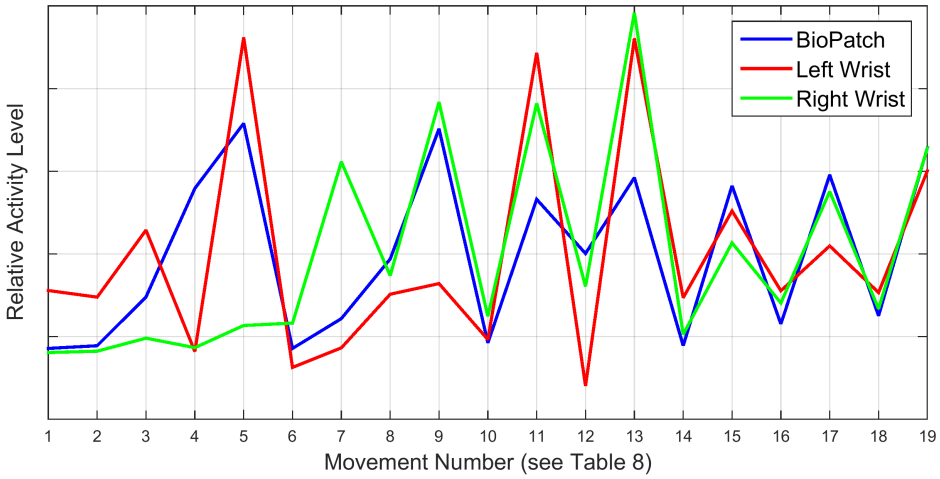

Figure 42. Relative Activity Levels of Accelerometers

Table 8. Description of Movement Numbers

Movement Number	Type	Distance	Speed
1	None	None	None
2	Left Arm	Short	Slow
3			Fast
4		Long	Slow
5			Fast
6	Right Arm	Short	Slow
7			Fast
8		Long	Slow
9			Fast
10	Both Arms	Short	Slow
11			Fast
12		Long	Slow
13			Fast
14	Left Leg	Short	Slow
15		Long	Fast
16	Right Leg	Long	Slow
17			Fast
18	Both Legs	Long	Slow
19			Fast

As the graph shows, the activity of the left wrist accelerometer increases with larger movements and more activity of the left arm. It shows little activity when only the right arm is moving, but shows moderate activity when the legs are moving. The same is true for the right wrist accelerometer. Interestingly, the BioPatch detects most movement in the arms and legs. It does not seem to notice small, light movements of the arms, but it detects most movements of the legs. These results suggest that the BioPatch can be used to measure stillness during float sessions. More research is needed to determine thresholds that can be used to distinguish between types of body movements.

6.2 Avoidance

Avoidance behavior was characterized in a brief experiment using the Kinect since some float studies seek to examine it in participants exposed to certain stimuli. During the float sessions, participants are held in place with the foothold system so that their heads remain in the same location. A stimulus can be delivered in various levels of intensity to the left, right, or center of the participant's head. In these tests, researchers want to determine if participants exhibit avoidance behavior by moving in the opposite direction of stimulus delivery.

Such an experiment is fitting for the Kinect since the foothold system is already required. To test the Kinect's ability to monitor avoidance behavior, a participant floated in the tank and moved his head to the left and right after collecting a baseline measure of head position. The first of these movements was made by simply rotating

the head left and right while keeping the rest of the body still. The second test required the participant to move his entire body left and right while keeping his feet on the foothold system. With small head movements, the x-coordinate of the head ranged from 219 to 278 pixels. For large movements, it ranged from 162 to 327 pixels. This confirmed that the Kinect can detect both types of head movements, and the reported locations can be used to measure avoidance.

One simple measure of avoidance is distance traveled from the center or baseline position. The participant was able to move his head left or right 29.5 pixels from the center for the experiment with small head movements and 82.5 pixels left and right with large movements. Such travel distances can be separated into categories and used to define varying levels of avoidance.

Avoidance can also be characterized in degrees shifted away from the centerline. Using the neck or waist as a hinge point, the head location can be used to measure how many degrees it is away from the centerline. This again can be broken into categories to describe multiple levels of avoidance. Since values will vary from person to person based on body type, future research should investigate methods to standardize these measures across participants.

Chapter 7: Conclusion

Float tanks are returning as a form of therapeutic treatment in many recreational and healthcare settings. This thesis presented the selection and validation of off-the-shelf biosensors to aid researchers and float tank entrepreneurs investigate the effects of this novel healthcare environment. Modifications to the selected devices were developed to ensure usability in the unique environment created by float tanks, and these modifications were tested to determine their effectiveness in protecting the devices and minimizing invasiveness. After an initial process of validation, it was determined that the modified biosensors could successfully and continually monitor movement, ECG, respiration, EEG, and blood pressure during float sessions.

After initial validation, a protocol and two techniques were developed to ensure time synchronization between devices. These were tested against an industry-leading physiological recording device, and the results verified the effectiveness of the methods to ensure accuracy of the biosensors' timestamps. Additional experiments between devices further validated the methods and illustrated how an event can be identified in multiple data streams. Additionally, an artificial neural network was designed to automatically detect R-peaks in ECG signals. This gives researchers full access to the ECG data, enabling them to calculate cardiac metrics as they see fit. Using accelerometer data from two devices, optimal cut-points were determined to classify movement and establish a measure of stillness for float research.

Future work should focus on determining the invasiveness of each biosensor. Such a study would reveal which devices or combination of devices remove participants from the float experience. Other research could develop more efficient methods of finding R-peaks in ECG signals. Since the accuracy of automatic detectors can only be calculated after collecting ground-truth data, an automated method of annotating R-peaks would help provide more training data for a neural network or other machine-learning agents. Improvements are also needed to design better algorithms for detecting movement. Lastly, data from various sensors should be combined into patient reports. One of the goals of float research is to develop treatments for mentally ill patients, and reports would empower patients to take ownership of their treatment by tracking their progress.

Float research will also benefit from advancements in industry. Personal health devices are becoming more available, but manufacturers need to improve their devices' abilities to synchronize with devices of other companies. This may be solved by utilizing a common platform or tool to collect and analyze data from multiple biosensors. Allowing users to easily and flexibly insert timestamps into each data stream would also aid the synchronization process. Companies designing biosensors specifically for the float environment should strive to fully waterproof their devices and limit points of entrance by implementing wireless charging and data transmission. Although physiological monitoring devices have progressed greatly since flotation research began, many tested in this thesis still failed to survive in the float tank's harsh environment. Nevertheless, this work presented the first successful implementation of collecting continuous physiological data during the float experience.

References

[1] J. T. Shurley, "Profound Experimental Sensory Isolation," *Am. J. Psychiatry*, vol. 117, no. 6, pp. 539–545, Dec. 1960.

[2] J. C. Lilly and J. T. Shurley, "Experiments in Solitude in Maximum Achievable Physical Isolation with Water Suspension of Intact Healthy Persons," *Psychophysiological Asp. Sp. Flight*, pp. 238–247, 1961.

[3] J. W. Turner and T. H. Fine, "Effects of relaxation associated with brief restricted environmental stimulation therapy (REST) on plasma cortisol, ACTH, and LH," *Biofeedback Self. Regul.*, vol. 8, no. 1, pp. 115–126, 1983.

[4] J. W. Turner and T. H. Fine, "Restricting environmental stimulation influences levels and variability of plasma cortisol," *J. Appl. Physiol.*, vol. 70, no. 5, pp. 2010–2013, 1991.

[5] D. G. Forgays and M. J. Belinson, "Is Flotation Isolation a Relaxing Environment?," *J. Environ. Psychol.*, no. April 1983, pp. 19–34, 1986.

[6] A. Barabasz, M. Barabasz, R. Dyer, and N. Rather, "Effects of Chamber REST, Flotation REST and Relaxation on Transient Mood State," in *Clinical and Experimental Restricted Environmental Stimulation*, New York, NY: Springer New York, 1993, pp. 113–120.

[7] S. Å. Bood, U. Sundequist, A. Kjellgren, T. Norlander, L. Nordström, K. Nordenström, and G. Nordström, "Eliciting the relaxation response with the help of flotation-rest (restricted environmental stimulation technique) in patients with stress-related ailments.," *International Journal of Stress Management*, vol. 13, no. 2. pp. 154–175, 2006.

[8] T. H. Fine and J. W. Turner, "The effect of brief restricted environmental stimulation therapy in the treatment of essential hypertension," *Behav. Res. Ther.*, vol. 20, no. 6, pp. 567–570, 1982.

[9] D. S. O'Leary and R. L. Heilbronner, "Flotation REST and Information Processing: A Reaction Time Study," in *Restricted Environmental Stimulation*, 1990, pp. 113–124.

[10] G. D. Jacobs, R. L. Heilbronner, and J. M. Stanley, "The effects of short term flotation REST on relaxation: a controlled study.," *Health Psychol.*, vol. 3, no. 2, pp. 99–112, 1984.

[11] J. W. Turner, W. Gerard, J. Hyland, P. Nieland, and T. H. Fine, "Effects of Wet and Dry Flotation REST on Blood Pressure and Plasma Cortisol," in *Clinical and*

Experimental Restricted Environmental Stimulation, 1993, pp. 239–247.

[12] D. van Dierendonck and J. Te Nijenhuis, "Flotation restricted environmental stimulation therapy (REST) as a stress-management tool: A meta-analysis," *Psychol. Health*, vol. 20, no. 3, pp. 405–412, 2004.

[13] S. A. Bood, U. Sundequist, A. Kjellgren, G. Nordstrom, and T. Norlander, "Effects of flotation-restricted environmental stimulation technique on stress-related muscle pain: What makes the difference in therapy - Attention-placebo or the relaxation response?," *Pain Res. Manag.*, vol. 10, no. 4, pp. 201–209, 2005.

[14] S. Å. Bood, U. Sundequist, A. Kjellgren, G. Nordström, and T. Norlander, "Effects of Flotation Rest (Restricted Environmental Stimulation Technique) on Stress Related Muscle Pain: Are 33 Flotation Sessions More Effective Than 12 Sessions?," *Soc. Behav. Personal. an Int. J.*, vol. 35, no. 2, pp. 143–156, 2007.

[15] J. W. Turner, T. Fine, G. Ewy, P. Sershon, and T. Freundlich, "The presence or absence of light during flotation restricted environmental stimulation: Effects on plasma cortisol, blood pressure, and mood," *Biofeedback Self. Regul.*, vol. 14, no. 4, pp. 291–300, 1989.

[16] G. Ewy, P. Sershon, and T. Freundlich, "The Presence or Absence of Light in the REST Experience: Effects on Plasma Cortisol, Blood Pressure and Mood," in *Restricted Environmental Stimulation*, 1990, pp. 93–104.

[17] T. Fine, J. W. Turner, and A. McGrady, "Effects of Biobehaviorally Assisted Relaxation Training on Blood Pressure and Hormone Levels," in *Restricted Environmental Stimulation*, 1990, pp. 184–201.

[18] D. G. Forgays, D. K. Forgays, M. Pudvah, and D. Wright, "A Direct Comparison of the 'Wet' and 'Dry' Flotation Environments," *J. Environ. Psychol.*, pp. 179–187, 1991.

[19] G. D. Steel, "Relaxed and Alert: Patterns of T-wave amplitude and heart rate in a REST environment," 1988.

[20] P. M. Morgan, A. J. Salacinski, and M. A. Stults-Kolehmainen, "The acute effects of flotation restricted environmental stimulation technique on recovery from maximal eccentric exercise.," *J. strength Cond. Res. Strength Cond. Assoc.*, vol. 27, no. 12, pp. 3467–3474, 2013.

[21] E. A. Serafetinides, J. T. Shurley, R. Brooks, and W. P. Gideon, "Electrophysiological changes in humans during sensory isolation," *Aerosp. Med.*, vol. 42, no. 8, pp. 840–842, 1971.

[22] T. Fine, D. Mills, and J. Turner, "Differential Effects of Wet and Dry Flotation REST on EEG Frequency and Amplitude," in *Clinical and Experimental Restricted Environmental Stimulation*, New York, NY: Springer New York,

1993, pp. 205–213.

[23] AAMI, *ANSI/AAMI/ISO 81060-1:2007/(R)2013 - Non-invasive sphygmomanometers - Part 1: Requirements and test methods for non-automated measurement type*. 2013.

[24] AAMI, *ANSI/AAMI/ISO 81060-2:2013 - Non-invasive sphygmomanometers - Part 2: Clinical investigation of automated measurement type*. 2013.

[25] AAMI, *ANSI/AAMI EC38:2007: Medical electrical equipment – Part 2-47 : Particular requirements for the safety , including essential performance , of ambulatory electrocardiographic systems Objectives and uses of AAMI standards and recommended practices*. 2007.

[26] D. W. Esliger, A. V. Rowlands, T. L. Hurst, M. Catt, P. Murray, and R. G. Eston, "Validation of the GENEA accelerometer," *Med. Sci. Sports Exerc.*, vol. 43, no. 6, pp. 1085–1093, 2011.

[27] W. A. Welch, D. R. Bassett, P. S. Freedson, D. John, J. A. Steeves, S. A. Conger, T. G. Ceaser, C. A. Howe, and J. E. Sasaki, "Cross-validation of waist-worn GENEA accelerometer cut-points," *Med. Sci. Sports Exerc.*, vol. 46, no. 9, pp. 1825–1830, 2014.

[28] D. John, J. Sasaki, J. Staudenmayer, M. Mavilia, and P. S. Freedson, "Comparison of raw acceleration from the GENEA and ActiGraph??? GT3X+ activity monitors.," *Sensors (Basel).*, vol. 13, no. 11, pp. 14754–14763, 2013.

[29] J. J. B. Allen, A. S. Chambers, and D. N. Towers, "The many metrics of cardiac chronotropy: A pragmatic primer and a brief comparison of metrics," *Biol. Psychol.*, vol. 74, no. 2, pp. 243–262, 2007.

[30] D. L. Mills, "Internet Time Synchronization: The Network Time Protocol," *IEEE Trans. Commun.*, vol. 39, no. 10, pp. 1482–1493, 1991.

[31] BIOPAC, "How Do I Sync My Stimulus Presentation Software with my Data Acquisition Software?" [Online]. Available: https://www.biopac.com/knowledge-base/how-do-i-sync-my-stimulus-presentation-software-with-my-data-acquisition-software/. [Accessed: 12-Feb-2015].

[32] J. Shotton, A. Fitzgibbon, M. Cook, T. Sharp, M. Finocchio, R. Moore, A. Kipman, and A. Blake, "Real-time Human Pose Recognition in Parts from Single Depth Images," *Stud. Comput. Intell.*, vol. 411, pp. 119–135, 2013.

[33] J. Putz-Leszczynska and M. Granacki, "Gait biometrics with a Microsoft Kinect sensor," in *2014 International Carnahan Conference on Security Technology (ICCST)*, 2014, vol. 360, pp. 1–5.

[34] P. J. . Noonan, J. . Howard, T. F. . Cootes, W. A. . Hallett, and R. . Hinz, "Realtime Markerless Rigid Body Head Motion Tracking Using the Microsoft Kinect," *IEEE Nucl. Sci. Symp. Conf. Rec.*, pp. 2241–2246, 2012.

[35] I. This, Z. Technology, and T. Bioharness, "Validity of BioHarness ™ Heart Rate vs 3-lead ECG Validity of BioHarness ™ Heart Rate vs 3-lead ECG," *Technology*, pp. 3–4, 2008.

[36] J. A. Johnstone, P. A. Ford, G. Hughes, T. Watson, and A. T. Garrett, "Bioharness™ multivariable monitoring device. Part I: Validity," *J. Sport. Sci. Med.*, vol. 11, no. 3, pp. 400–408, 2012.

[37] J. A. Johnstone, P. A. Ford, G. Hughes, T. Watson, and A. T. Garrett, "Bioharness™ multivariable monitoring device. Part II: Reliability," *J. Sport. Sci. Med.*, vol. 11, no. 3, pp. 409–417, 2012.

[38] B. A. Reyes, H. F. Posada-Quintero, J. R. Bales, A. L. Clement, G. D. Pins, A. Swiston, J. Riistama, J. P. Florian, B. Shykoff, M. Qin, and K. H. Chon, "Novel electrodes for underwater ECG monitoring," *IEEE Trans. Biomed. Eng.*, vol. 61, no. 6, pp. 1863–1876, 2014.

[39] R. Treskes, E. Van Der Velde, D. Eindhoven, and M. Schalij, "Comparison of Four Smartphone Compatible Blood Pressure Monitors Methods Blood pressure monitors," *Comput. Cardiol. (2010).*, pp. 637–640, 2015.

[40] D.-H. Kim, N. Lu, R. Ma, Y.-S. Kim, R.-H. Kim, S. Wang, J. Wu, S. M. Won, H. Tao, A. Islam, K. J. Yu, T. Kim, R. Chowdhury, M. Ying, L. Xu, M. Li, H.-J. Chung, H. Keum, M. McCormick, P. Liu, Y.-W. Zhang, F. G. Omenetto, Y. Huang, T. Coleman, and J. A. Rogers, "Epidermal electronics.," *Science*, vol. 333, no. 6044, pp. 838–43, Aug. 2011.

[41] Microsoft, "Kinect for Windows Sensor Components and Specifications." [Online]. Available: https://msdn.microsoft.com/en-us/library/jj131033.aspx?f=255&MSPPError=-2147217396.

[42] Activinsights, "GENEActiv Instructions." p. 29, 2012.

[43] Zephyr, "Log Data Descriptions." p. 38, 2013.

[44] QardioArm, "QardioArm User Manual." p. 7.

[45] H. M. Wang and S. C. Huang, "SDNN/RMSSD as a surrogate for LF/HF: A revised investigation," *Model. Simul. Eng.*, vol. 2012, 2012.

[46] J. Ma, C. Shi, Z. Zhang, J. Zhu, and L. Wang, "A Differentiation-based Adaptive Double Threshold Method for Real Time Electrocardiogram R peak Detection," no. Bmei, pp. 259–263, 2014.

[47] J. Fernandez, M. Harris, and C. Meyer, “Combining algorithms in automatic detection of R-peaks in ECG signals,” *18th IEEE Symp. Comput. Med. Syst.*, pp. 0–5, 2005.

[48] S. M. Szilagyi, “Comparison of the neural-network-based adaptive filtering andwavelet transform for R, T and P waves detection,” *Inf. Technol. Appl. Biomed. ITAB ’97. Proc. IEEE Eng. Med. Biol. Soc. Reg. 8 Int. Conf.*, pp. 73–75, 1997.

[49] Q. Xue, Yu Hen Hu, and W. J. Tompkins, “Neural-network-based adaptive matched filtering for QRS detection,” *IEEE Trans. Biomed. Eng.*, vol. 39, no. 4, pp. 317–329, 1992.

[50] M. A. Hasan, M. I. Ibrahimy, and M. B. I. Reaz, “NN-based R-peak detection in QRS complex of ECG signal,” *IFMBE Proc.*, vol. 21 IFMBE, no. 1, pp. 217–220, 2008.

[51] M. H. Hassoun, *Fundementals of Artificial Neural Networks*. MIT Press.

[52] M. Borges, “peakdet.” 2014.